Vibration and Acoustics Research Journal
Vol. 1, No. 1; 2019
Published by CanSRG
http://cansrg.com/journals/varj/

Implementation of the KDamper as a Stiff Seismic Absorption Base: A Preliminary Assessment

Konstantinos A. Kapasakalis[1,*], Ioannis A. Antoniadis[2] and Evangelos J. Sapountzakis[1]

[1]*Institute of Structural Analysis and Antiseismic Research, School of Civil Engineering, National Technical University of Athens, Zografou Campus GR-157 80, Athens, Greece.*
[2]*Dynamics and Structures Laboratory, Mechanical Engineering Department, National Technical University of Athens, Zografou Campus GR-157 80, Athens, Greece.*

Abstract

This study proposes a novel base isolation approach, based on the KDamper concept. The KDamper is a passive vibration absorption concept, based essentially on the optimal combination of appropriate stiffness elements, one of which has a negative value. A spectra driven optimization of the KDamper nominal frequency for implementation in a typical 3-story concrete building structure is proposed. The effect of the KDamper nominal frequency to the system transfer functions, power spectral densities, and root mean square responses are examined. Two alternative options for the implementation of the KDamper are considered. In the first one, the nominal KDamper frequency is selected equal to the low frequency of a conventional base isolation system, resulting in a drastic improvement of the superstructure dynamic performance. The second one foresees the implementation of the KDamper with a much higher nominal frequency. This leads to a drastic reduction of the base relative displacement, in the order of a few centimeters, combined with an acceptable superstructure dynamic behavior. The results are evaluated in the time domain and indicative designs of the KDamper devices prove that the stiffness values, as well as the additional mass and the artificial damper, are within reasonable technological capabilities. Finally, it is proven that the results of the non-linear proposed configuration are in a very good agreement to that of the initial linear problem. As a consequence, the KDamper can be implemented as a "stiff seismic absorption base", as an alternative to conventional base isolation approaches.

Keywords: *Vibration Control; Negative Stiffness; Seismic Protection; KDamper.*

1. Introduction

In response to the damage generated by earthquakes occurring in densely populated areas, seismic design codes for buildings, bridges, and infrastructure changed towards the design of structures with better seismic performance. Seismic isolation appears to be the most promising alternative to conventional antiseismic techniques, as it is based on the concept of reducing the seismic demand rather than increasing the earthquake resistance capacity of the structure [1]. Isolation systems in the bases of the structures essentially provide horizontal isolation from the effects of earthquake shaking, by decoupling the superstructure from base-foundation during earthquakes. In this context, a variety of isolation devises including elastomeric bearings (with and without lead core) [2] frictional/sliding bearings, roller bearings and most recently TMD devices, has been developed. Furthermore, the significant advance of mechanical expertise has facilitated the implementation of more complex devices, such as newly-fabricated hardware incorporating negative stiffness elements.

* Corresponding author
Submitted: August 2, 2019 Accepted: December 20, 2019

Tuned Mass Dampers (TMDs) consists perhaps the most popular and mature approach, among the large variety of active and passive control strategies. The TMD concept was first applied by Frahm [3], whereas an optimal design theory for such configurations has been proposed by Den Hartog [4]. Since then, TMDs have been employed on a vast array of systems with skyscrapers being among the most interesting ones [5-8]. More recently, the use of TMDs has been included in studies concerning mitigation of the effects of seismic or other kinds of excitation on bridge structures [9]. The natural frequency of the TMD is tuned in resonance with the fundamental mode of the primary structure. Thus, a large amount of the structural vibrating energy is transferred to the TMD and then dissipated by damping. Besides the effectiveness of such devices, TMDs suffer from two main disadvantages: a) environmental influences and other external parameters may alter the TMD properties, disturbing its tuning and lead to deterioration of the device's performance [10], and b) a large oscillating mass is required in order to achieve significant vibration reduction rendering its construction and placement procedure rather difficult.

The last steps towards vibration absorption include the introduction of negative stiffness elements (Negative Stiffness Devices and "Quazi Zero Stiffness" oscillators) to seismic isolation mechanisms. True negative stiffness is defined as a force that assists motion instead of opposing it as in the case of positive stiffness elements. Starting from the work of Molyneaux [11] and Platus [12], the basic idea behind the incorporation of negative stiffness elements is the significant reduction of the stiffness that consequently leads to the reduction of the natural frequency of the system even at almost zero levels, as in Carrela et al. [13] being thus called "Quazi Zero Stiffness" (QZS) oscillators. Enhanced vibration isolation is, thus, achieved due to the fact that the transmissibility of the system for all operating frequencies above the natural one is reduced. An initial comprehensive review of such designs can be found in Ibrahim [14]. The negative stiffness behavior is primarily achieved by special mechanical designs involving conventional positive stiffness pre-stressed elastic mechanical elements, such as post-buckled beams, plates, shells and pre-compressed springs, arranged in appropriate geometrical configurations. Some interesting designs are described in [15-16]. Among others, QZS oscillators find numerous applications in seismic isolation [17-24].

The novel KDamper concept introduced by Antoniadis et al. [25] combines the beneficial characteristics of both Negative Stiffness Elements and Tuned Mass Dampers. The proposed device can exhibit extraordinary damping properties, without the drawbacks of TMDs or QZS oscillators. The novelty of the KDamper concept lies in the appropriate redistribution of the individual stiffness elements and the reallocation of damping. The inherent instability that usually accompanies configurations with negative stiffness elements is hereby avoided, as the proposed device is designed to be both statically and dynamically stable. The additional mass of the KDamper operates similar to the additional mass of the TMDs. However, the KDamper overcomes the sensitivity problems of TMDs, as the tuning is mainly controlled by the negative stiffness element. Once such a system's parameters are selected optimally, the isolated system exhibits a significantly improved dynamic and damping behavior. The procedure for the optimal selection of the KDamper parameters can follow the classical minmax ($H\infty$) approach, first proposed by Den Hartog [4]. Relevant procedures are described in Antoniadis et al. [25] for force excitation/displacement response transfer function and in [26-29] for base acceleration excitation/relative structure displacement response transfer function. An alternative design approach, incorporating an optimization algorithm, can be found in Syrimi et al. [30].

This paper examines the feasibility of the implementation of the KDamper as a seismic absorption

base in a typical 3-story concrete building structure. The objective is to optimally select the KDamper parameters with respect to the provisions of the design spectra of the various seismic codes and to assess the resulting benefits to the dynamic behavior of the structure. Initial approaches towards the implementation of the KDamper as a seismic absorption/damping base of structures are considered. A database of artificial accelerograms is generated, designed to be compatible with a rather conservative seismic case corresponding to EC8, Class C. The mean acceleration response spectrum is calculated, matching accurately the EC8 response spectra. The least-square fitting of the mean power spectral density is calculated and used as the ground motion excitation acceleration PSD. The response power spectral densities are formed and the root mean square responses are derived, as an indicator of the actual energy content of the response. A spectra driven optimization of the KDamper nominal frequency, for the implementation in a typical 3-story concrete building structure, is considered. The transfer functions, response power spectral densities, and root mean square responses are formed and alternative options for the implementation of the KDamper are considered. Numerical evaluation is made for the implementation of the KDamper concept as a seismic absorption/damping base. Initially, the system's parameters are selected and a linear problem is first solved in order to estimate the maximum displacement values that are necessary for the design of the stiffness elements, the additional mass, and the artificial damper. Finally, the KDamper devices are designed and the non-linear problem is solved.

The essential features and novel aspects of the current paper are

1. The optimal design of the KDamper, for optimization of the structure absolute acceleration transfer function, provides an improved dynamic behavior, as compared to other transfer functions previously used.
2. The KDamper is implemented as a seismic absorption/damping base for the seismic protection of structures.
3. A compatible ground motion excitation acceleration PSD is used to define the root mean square (RMS) responses. The results confirm the ability of the RMS responses to represent accurately the effect of the variation of the nominal KDamper frequency to the system maximum dynamic responses.
4. The implementation of the KDamper is numerically evaluated, and the proposed configuration reveals a number of advantages, summarized as follows
    i. The indicative design of the KDamper devices proves that the additional mass, the artificial damper, and the stiffness elements, of each implemented device, are within reasonable technological capabilities.
    ii. The results of the non-linear problem are in a very good agreement to that of the initial linear problem.
    iii. The KDamper is implemented effectively as an alternative to the conventional seismic isolation approaches, greatly improving the dynamic behavior of the superstructure, while retaining the base displacement in the order of a few centimeters.

2. The KDamper as a Seismic Absorption Base

A brief overview of the novel KDamper concept and its basic properties can be found in Appendix A. The procedure for the optimal selection of the KDamper parameters follows the classical minmax (H∞) approach, first proposed by Den Hartog [4], considering base acceleration excitation/structure absolute acceleration transfer function minimization. A detailed description of

the optimization process can be found in Appendix B. In this section of the paper, the KDamper is implemented as a seismic absorption/damping base of a flexible structure, initially mounted on a fixed base and alternatively on a conventional or highly damped seismic isolation base.

2.1. Initial flexible structure on a fixed base

The initial fixed base flexible structure will be referred hereafter as FBS (fixed base structure). The equation of motion of the FBS (Figure 1.a) is

$$m_S\ddot{u}_S + c_S\dot{u}_S + k_S u_S = -m_S a_G \tag{1}$$

where $u_S = x_S - x_G$. The resulting transfer functions are

$$\tilde{H}_{US} = \tilde{U}_S / A_G = -\tilde{H}^{-1} m_S \; ; \; \tilde{H}_{AS} = \tilde{A}_S / A_G = (-\omega^2 \tilde{X}_S) / A_G = 1 - \omega^2 \tilde{H}_{US} \; ; \; \tilde{H} = [-\omega^2 m_S + j\omega c_S + k_S] \tag{2}$$

The natural frequency and the damping ratio of the FBS are defined as

$$\omega_S = \sqrt{k_S / m_S} \; ; \; \zeta_S = c_S / (2\omega_S m_S) \tag{3}$$

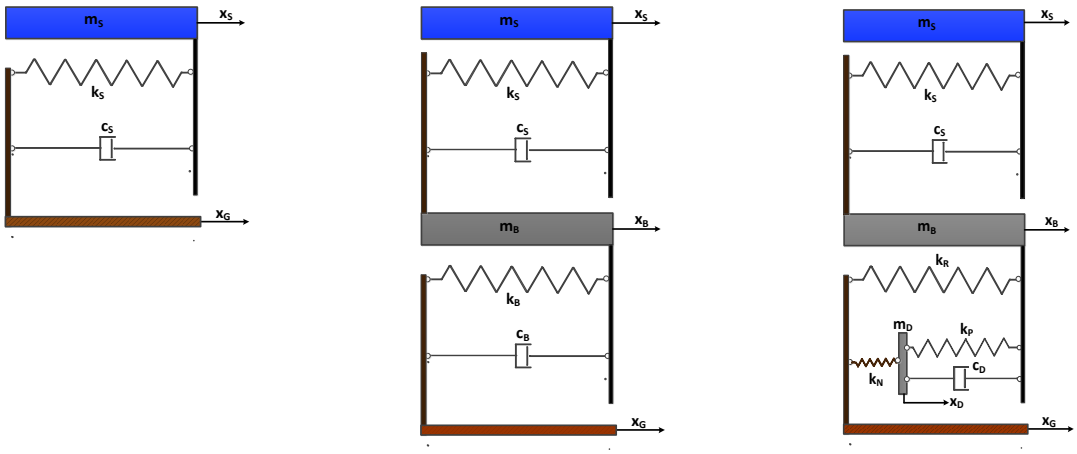

(a) (b) (c)

Figure 1. (a) Flexible structure on a fixed base, (b) flexible structure on a conventional or highly damped seismic isolation base and (c) possible implementation of KDamper as a seismic absorption/damping base.

2.2. Flexible structure on a seismic isolation base

The initial FBS is mounted on a seismic isolating base (Figure 1.b), assimilated to another SDoF system. The flexible structure on a seismic isolation base will be referred hereafter as BIS (base isolated structure). The equations of motion of the BIS are

$$m_S(\ddot{u}_S + \ddot{u}_B) + c_S\dot{u}_S + k_S u_S = -m_S a_G \tag{4.a}$$

$$m_B\ddot{u}_B + m_S(\ddot{u}_S + \ddot{u}_B) + c_B\dot{u}_B + k_B u_B = -(m_S + m_B) a_G \tag{4.b}$$

where $u_S = x_S - x_B$ and $u_B = x_B - x_G$. The transfer functions of this system are

$$\begin{bmatrix} \tilde{H}_{US} \\ \tilde{H}_{UB} \end{bmatrix} = \begin{bmatrix} \tilde{U}_S / A_G \\ \tilde{U}_B / A_G \end{bmatrix} = -\tilde{H}^{-1} \begin{bmatrix} m_S \\ m_S + m_B \end{bmatrix} \tag{5.a}$$

$$\tilde{H}_{AS} = \tilde{A}_S / A_G = 1 - \omega^2 (\tilde{H}_{US} + \tilde{H}_{UB}) \; ; \; \tilde{H}_{AB} = \tilde{A}_B / A_G = 1 - \omega^2 \tilde{H}_{UB} \tag{5.b}$$

The natural frequency and the damping ratio of the BIS are defined as

$$\omega_B = 2\pi f_B = \sqrt{k_B / M_{tot}} \; ; \; \zeta_B = c_B / (2\omega_B M_{tot}) \; ; \; M_{tot} = (1 + \mu_B) m_S \; ; \; \mu_B = m_B / m_S \tag{6}$$

The performance of the BIS system strongly depends on the selection of the natural frequency f_B, which is selected to be significantly lower than the natural frequency f_S of the structure.

2.3. The KDamper as a seismic absorption/damping base

Among the large variety of possibilities, the KDamper can be implemented for seismic protection as an alternative (or supplement) of a conventional seismic isolation base. The implementation of the KDamper as a seismic absorption/damping base will be referred hereafter as KDAB (KDamper absorption base). The corresponding configuration is shown in Figure 1.c, and the equations of motion of this system are

$$m_S(\ddot{u}_S+\ddot{u}_B)+c_S\dot{u}_S+k_S u_S=-m_S a_G \tag{7.a}$$

$$m_B\ddot{u}_B+m_S(\ddot{u}_S+\ddot{u}_B)+c_D(\dot{u}_B-\dot{u}_D)+k_P(u_B-u_D)+k_R u_B=-(m_S+m_B)a_G \tag{7.b}$$

$$m_D\ddot{u}_D-c_D(\dot{u}_B-\dot{u}_D)-k_P(u_B-u_D)+k_N u_D=-m_D a_G \tag{7.c}$$

where $u_D = x_D - x_G$. The transfer functions of this system are

$$\begin{bmatrix}\tilde{H}_{US}\\ \tilde{H}_{UB}\\ \tilde{H}_{UD}\end{bmatrix}=\begin{bmatrix}\tilde{U}_S/A_G\\ \tilde{U}_B/A_G\\ \tilde{U}_D/A_G\end{bmatrix}=-\tilde{H}^{-1}\begin{bmatrix}m_S\\ m_S+m_B\\ m_D\end{bmatrix} \tag{8.a}$$

$$\tilde{H}_{AS}=\tilde{A}_S/A_G=1-\omega^2(\tilde{H}_{US}+\tilde{H}_{UB});\ \tilde{H}_{AB}=\tilde{A}_B/A_G=1-\omega^2\tilde{H}_{UB};\ \tilde{H}_{AD}=\tilde{A}_D/A_G=1-\omega^2\tilde{H}_{UD} \tag{8.b}$$

$$\tilde{H}=\begin{bmatrix}-\omega^2 m_S+j\omega c_S+k_S & -\omega^2 m_S & 0\\ -\omega^2 m_S & -\omega^2(m_S+m_B)+j\omega c_D+k_P+k_R & -(j\omega c_D+k_P)\\ 0 & -(j\omega c_D+k_P) & -\omega^2 m_D+j\omega c_D+k_P+k_N\end{bmatrix} \tag{8.c}$$

The natural frequencies of the subsystems and the damping ratio of the KDAB are defined as

$$\omega_0=2\pi f_0=\sqrt{k_0/(m_S+m_B)};\ \omega_D=\sqrt{(k_P+k_N)/\mathrm{m}_D};\ \zeta_D=c_D/(2\omega_D m_D);\ k_0=k_R+\frac{k_P k_N}{k_P+k_N} \tag{9}$$

The parameters $m_B = \mu_B m_S$ and $m_D = \mu_D m_S$ depend on the base's and the damper's mass ratios respectively, μ_B and μ_D. The performance of the KDAB system strongly depends on the selection of the natural frequency f_0. However, this frequency does not necessarily need to be selected significantly lower than the natural frequency f_s of the structure, as in the case of the BIS.

3. Compatible Ground Motion Spectra, Response Power Spectral Densities, and Mean Square Responses

According to seismic design codes, the structure relative displacement, or acceleration, is within specified limits for a specific fundamental structure period and damping ratio. These limits strongly depend on the specific ground conditions and expected seismic intensity, as well as on the fundamental structural period, thus resulting in the so-called "Design Response Spectra". A typical form of these spectra is depicted in Figure 2.

The implementation of the KDamper leads to MDoF systems with multiple frequencies. Therefore, the direct application of this approach to the selection of the KDamper parameters is not possible. For this reason, time history analysis is required for the optimal design of the KDamper. Strong earthquake time histories are generated from one of three fundamental types of accelerograms: synthetic records obtained from seismological models, real accelerograms recorded in earthquakes (not all soil combinations are covered, not smoothed spectra) and artificial records, compatible with a specific design response spectrum, with the latter being the most suitable for code-based design.

Towards this direction, the generation of design response spectrum compatible ground acceleration excitations is necessary. This is far from being a trivial task, with rich background research, overviews of which can be found among others in [31-32]. There are numerous reasons behind

that, such as the fact that earthquakes are transients with non-stationary spectra and uncertain duration, as well as the fact that the design response spectra represent peak values of the response variables in the time domain which are quite difficult to match with spectral values in the frequency domain. For this reason, the approach followed in this paper is based on first generating a sample of artificial accelerograms whose response spectra is closely compatible with the design response spectra (EC8). Artificial spectrum-compatible accelerograms can be generated using SeismoArtif Software [33]. The artificial accelerograms used in this paper are designed to match a rather conservative but realistic case: the EC8 response spectra for a specific ground type, in this case, ground type C, for spectral acceleration 0.36 *g*, spectrum type I and importance class II. In Figure 3.a, an Artificial Accelerogram is presented, using Artificial Accelerogram Generation and Adjustment calculation method, with an envelope shape by Saragoni and Hart [34].

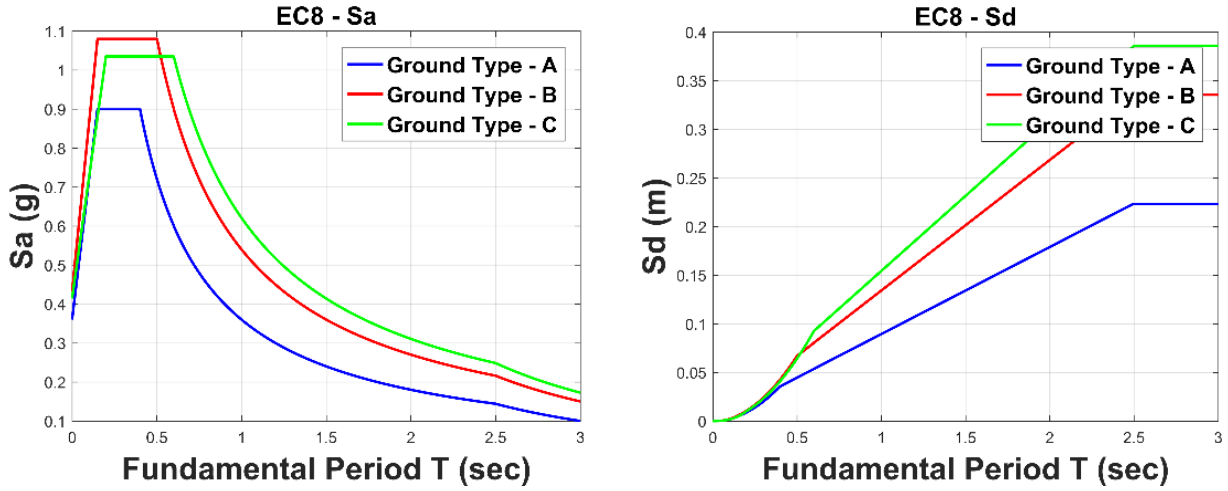

(a) (b)

Figure 2. EC8 Design response spectra: (a) Spectral acceleration and (b) Spectral displacement.

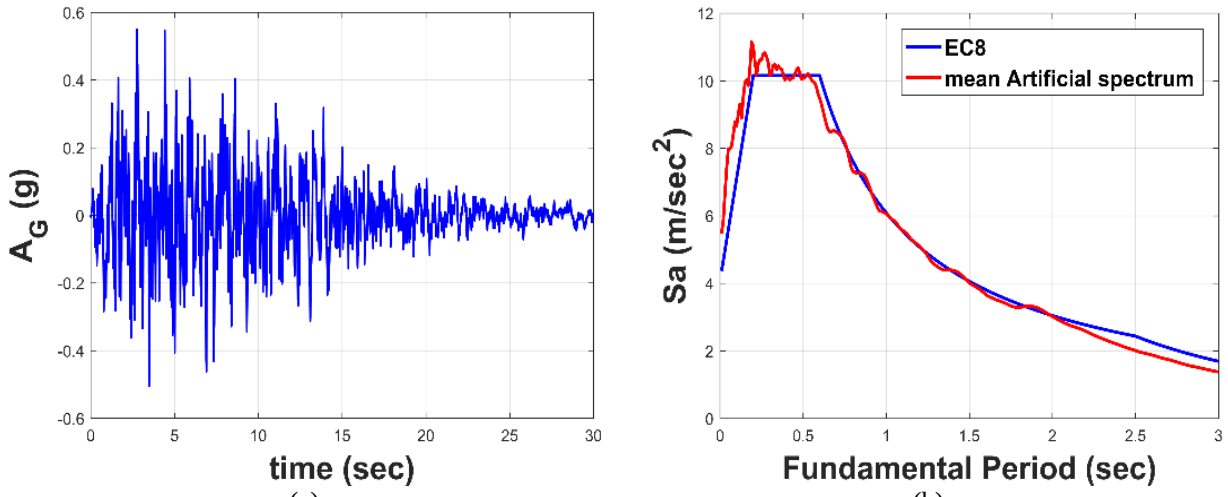

(a) (b)

Figure 3. (a) Artificial accelerogram and (b) mean artificial acceleration response spectra of 30 artificial accelerograms compared to the EC8 acceleration design response spectra.

The mean acceleration response spectrum is calculated and compared to the EC8 design response

spectrum. As observed in Figure 3.b, the mean acceleration response spectrum, for 30 artificial accelerograms, is matched very accurately with the EC8 response spectrum, with characteristics: spectral acceleration 0.36 *g*, ground type C, spectrum type I and importance class II. More specifically, the percentage deviation is under 10% in the range of periods from 0.2 to 2 *sec*, which is of actual concern.

The mean power spectral density S_{AM} of the 30 artificial accelerograms in the database is calculated, and presented in Figure 4.a, along with the least square fitting, which will be subsequently used as the ground motion excitation acceleration PSD S_A. Parallel, Figure 4.b presents a stationary power-spectral density function (red line) generated from [35] and adapted so that both spectral densities present the same peak value. A very good fit can be observed.

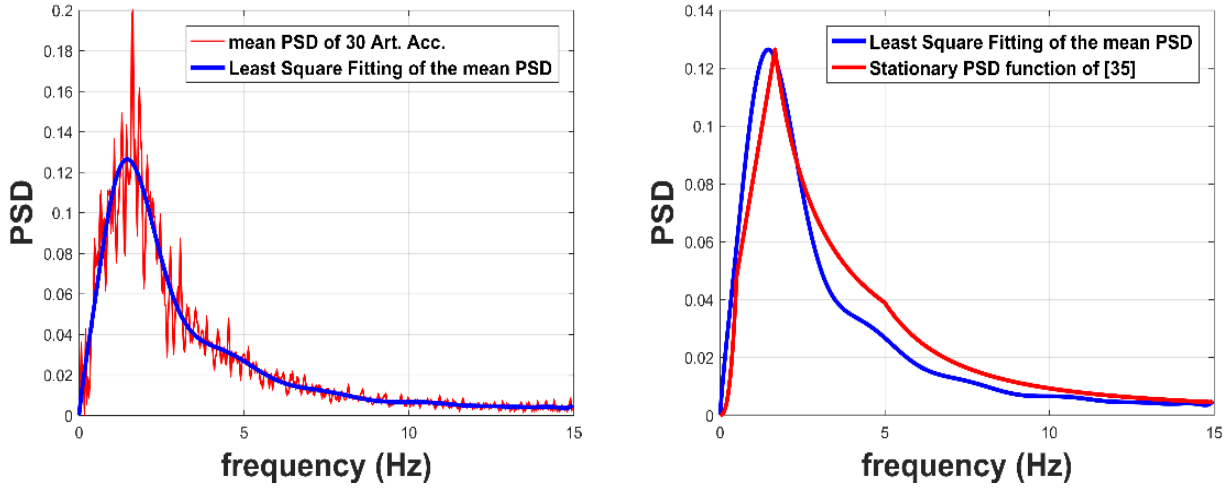

(a) (b)

Figure 4. (a) Mean power spectral density of the 30 artificial accelerograms in the database, S_{AM}, with the least square fitting S_A and (b) least-square fitting S_A compared with stationary power-spectral density function, as described in [35].

Having defined the ground motion excitation acceleration PSD S_A, the response power spectral densities, S_{US}, S_{UB}, S_{UD}, and S_{AS} of the system main responses can be derived as.

$$S_{US}(\omega) = H_{US}^2(\omega) S_A(\omega)\ ;\ S_{UB}(\omega) = H_{UB}^2(\omega) S_A(\omega)\ ;\ S_{UD}(\omega) = H_{UD}^2(\omega) S_A(\omega)\ ;\ S_{AS}(\omega) = H_{AS}^2(\omega) S_A(\omega) \quad (10)$$

where H_{US}, H_{UB}, H_{UD}, and H_{AS} are the transfer functions of the main system responses. It should be emphasized that the design response spectra of the seismic design codes (e.g. those in Figure 2), are entirely different than the response power spectral densities of Eq. (10). The root mean square value of the responses is defined next as the root of the area under the power spectral density curve, as an indication of the actual energy content of the response

$$R_{US} = \left[\int_{-\infty}^{+\infty} S_{US}(\omega)\,\mathrm{d}\omega\right]^{0.5};\ R_{UB} = \left[\int_{-\infty}^{+\infty} S_{UB}(\omega)\,\mathrm{d}\omega\right]^{0.5};\ R_{UD} = \left[\int_{-\infty}^{+\infty} S_{UD}(\omega)\,\mathrm{d}\omega\right]^{0.5};\ R_{AS} = \left[\int_{-\infty}^{+\infty} S_{AS}(\omega)\,\mathrm{d}\omega\right]^{0.5} \quad (11)$$

4. Spectra Driven Optimization of the KDamper Nominal Frequency for Implementation in a 3-Story Building Structure

A planar 3-story concrete building structure is considered, as sketched in Figure 5.a, in which the proposed vibration absorption concept, KDAB, is implemented as an alternative or supplement of the conventional base isolation approaches. A ground floor plan of a typical floor of the structure is presented in Figure 5.b. The assumptions made for the modeling of this structure are: the total

mass of the structure is concentrated at the floor levels, the slabs and grinders on the floors are rigid as compared to the columns, the columns are inextensible and weightless providing the lateral stiffness, the effect of soil-structure-interaction is not taken into consideration and the superstructure is considered to remain within the elastic limit during the seismic excitation.

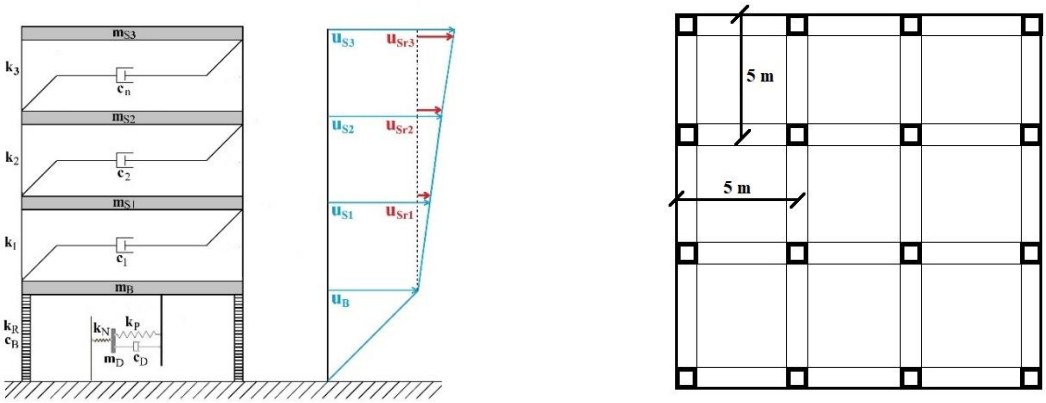

Figure 5. Examined 3-storey concrete building structure with the proposed absorption base system (KDAB), (a) sketch of the model and (b) typical ground floor plan of the structure.

As a result, the superstructure has 3 dynamic DoFs, represented by the relative to the base displacements of the 3-story masses m_{Sj} ($j=1, 2, 3$) (Figure 5.a), which are collected in the array $u_{sr}^T(t)=[u_{sr1}(t),\ u_{sr2}(t),\ u_{sr3}(t)]^T$. The equations of motion Eq. (7) still, hold, but now expressed in a matrix form and involving matrices having dimensions 5×5, in particular

$$[M][\ddot{u}(t)]+[C][\dot{u}(t)]+[K][u(t)]=-[\tau]a_G(t) \tag{12}$$

where the matrices and vectors entering Eq. (12) are defined as

$$[K]=\begin{bmatrix}[K_S] & [0] & [0]\\ [0]^T & k_P+k_R & -k_P\\ [0]^T & -k_P & k_P+k_N\end{bmatrix};[C]=\begin{bmatrix}[C_S] & [0] & [0]\\ [0]^T & c_D+c_B & -c_D\\ [0]^T & -c_D & c_D\end{bmatrix};[u(t)]=\begin{bmatrix}[u_{st}](t)\\ u_B(t)\\ u_D(t)\end{bmatrix}$$

$$[M]=\begin{bmatrix}[M_S] & [M_S][\tau_S] & [0]\\ [\tau_S]^T[M_S] & m_{S,tot}+m_B & 0\\ [0]^T & 0 & m_D\end{bmatrix};[\tau]=\begin{bmatrix}[M_S][\tau_S]\\ m_{S,tot}+m_B\\ m_D\end{bmatrix};m_{S,tot}=\sum_{i=1}^{n}m_i \tag{13}$$

where [*MS*], [*CS*] and [*KS*] are the 3-dimensional matrices of mass, damping and stiffness of the superstructure as if it was on a fixed base, [τ_S] is the 3×1 influence vector of the superstructure associated with the ground motion $x_G(t)$, and [*0*] is a 3×1 vector of zero terms. The elastic modulus is considered $E=26000\ MN/m^2$ (typical of a reinforced concrete frame), the mass of the 3 floors is $m_i=80000\ kg$ ($i=1, 2, 3$). Applying the classical modal analysis to the superstructure leads to the following natural periods $T_{Si}\ [sec] = [0.495, 0.177, 0.122]$. The basement mass is assumed to be $m_B=50000\ kg$, resulting in a base mass ratio $\mu_B=0.2083$. The damping coefficients of the superstructure are assumed to be mass and stiffness proportional (Rayleigh damping) with $\zeta_{Si}=0.02$ ($i=1, 2, 3$).

In order to observe the effect of the nominal KDamper frequency to 1) the transfer functions 2) the response power spectral densities and 3) the root mean square responses, of the main system parameters, two cases are considered. In the first one, the nominal frequency of the KDAB is equal to the low frequency (0.4 *Hz*) of the BIS system. This case will be referred to hereafter as KDAB-

L (KDamper Absorption Base - Low frequency). In the second one, a stiffer base is considered, with a nominal KDamper frequency of 1 *Hz*, in order to examine if the large base displacements, that are required in the classical seismic isolation concepts, can be avoided. This case will be referred to hereafter as KDAB-H (KDamper Absorption Base - High frequency). The parameters of the KDAB-L and KDAB-H are presented in Table 1. Specific details for the optimal selection of the KDAB parameters can be found in Appendix B.

Table 1. Parameters of the KDAB-L and KDAB-H systems (L - low frequency, H - high frequency).

System	μ (%)	κ	ζ_D	ε (%)	f_0 (Hz)
KDAB-L	5	3.41	0.622	5	0.4
KDAB-H	5	3.41	0.622	5	1

4.1. Effect of the KDamper nominal frequency on the relative displacement and absolute acceleration transfer Functions

Figure 6 presents the transfer functions of the floor drifts and the floor absolute accelerations, of the initial as well as the controlled system with the KDAB concept. It is observed, that before and after the implementation of the KDamper, the first-floor drift and the top (3rd) floor absolute acceleration, present the worst dynamic behavior in all frequency range. Therefore, in the following, only the results concerning the first-floor drift and the top floor absolute acceleration will be presented. The KDAB-H system, with a nominal frequency of 1 *Hz*, significantly enhances the superstructure's dynamic behavior both in terms of floor drifts and absolute accelerations. The KDAB-L system, with a natural frequency equal to the low frequency of conventional base isolation systems (0.4 *Hz*), dramatically improves the floor drifts and absolute accelerations, as in the case of conventionally base isolated structures.

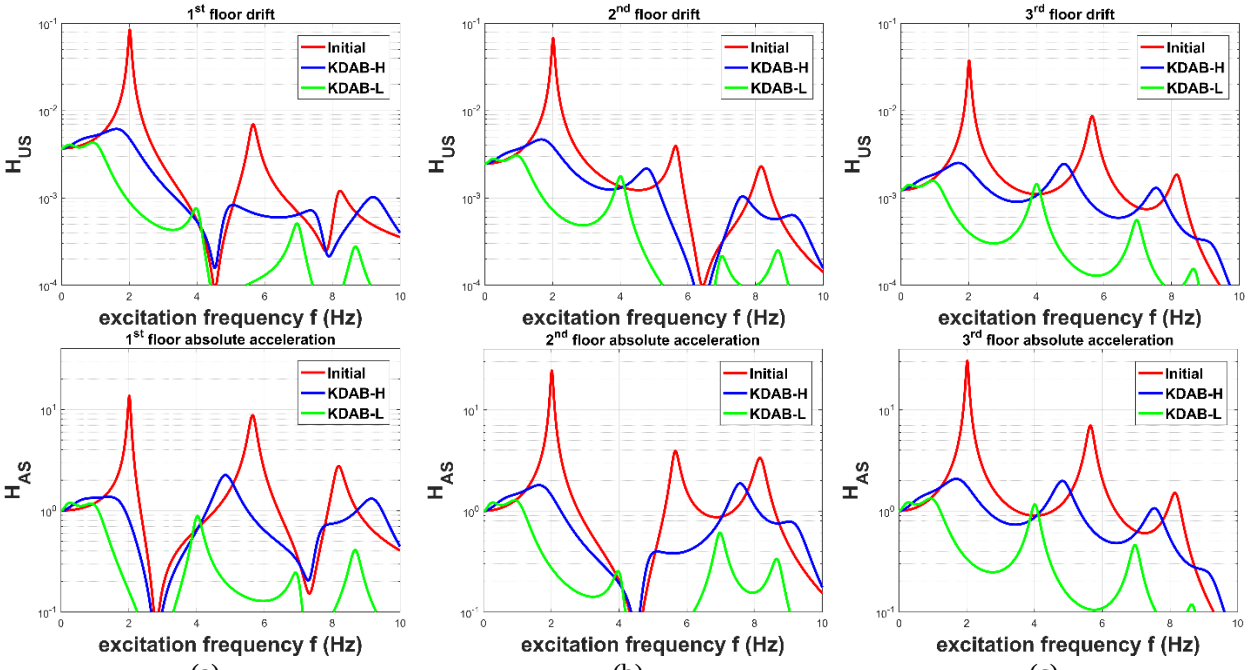

(a) (b) (c)

Figure 6. Transfer functions of the structure's floor drifts and absolute accelerations, (a) first floor, (b) second floor and (c) third floor, of the initial and the KDAB-L and KDAB-H systems.

By increasing the nominal frequency of the KDAB from 0.4 *Hz* (KDAB-L) to 1.0 *Hz* (KDAB-H),

the base's relative displacement, as well as the KDamper's relative displacement, are dramatically improved in all frequency range, as observed in Figure 7.

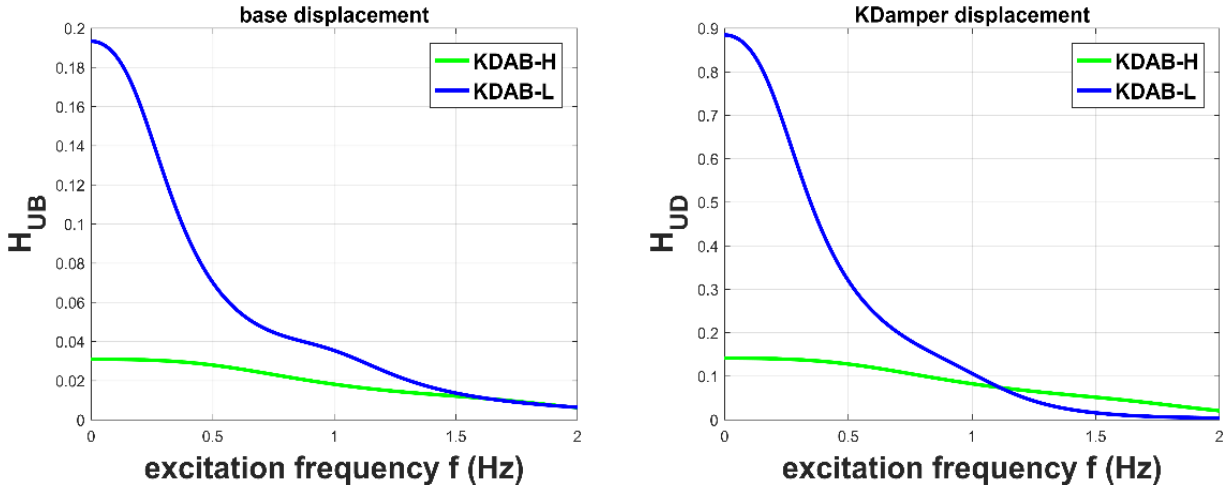

(a) (b)

Figure 7. Transfer functions of (a) base's relative displacement and (b) KDamper's relative displacement, of the KDAB-L and KDAB-H systems.

4.2. Effect of the KDamper nominal frequency on the response power spectral densities

Based on the design spectrum compatible ground motion acceleration excitation PSD S_A of Figure 4.a, the response power spectral densities of the initial system as well as the controlled structure with KDamper (KDAB system), are obtained and depicted in Figures 8 and 9. In Figure 8, the response power spectra densities S_{US} and S_{AS} of the 1st-floor drift and top floor (3rd) absolute acceleration, are presented. It is observed that the considered control systems (KDAB-L, and KDAB-H) manage to reduce the initial system's maximum values of the S_{US} and S_{AS} over two orders of magnitude. More specifically, the KDAB-L system always displays an improved behavior in all frequency range as compared with the KDAB-H system.

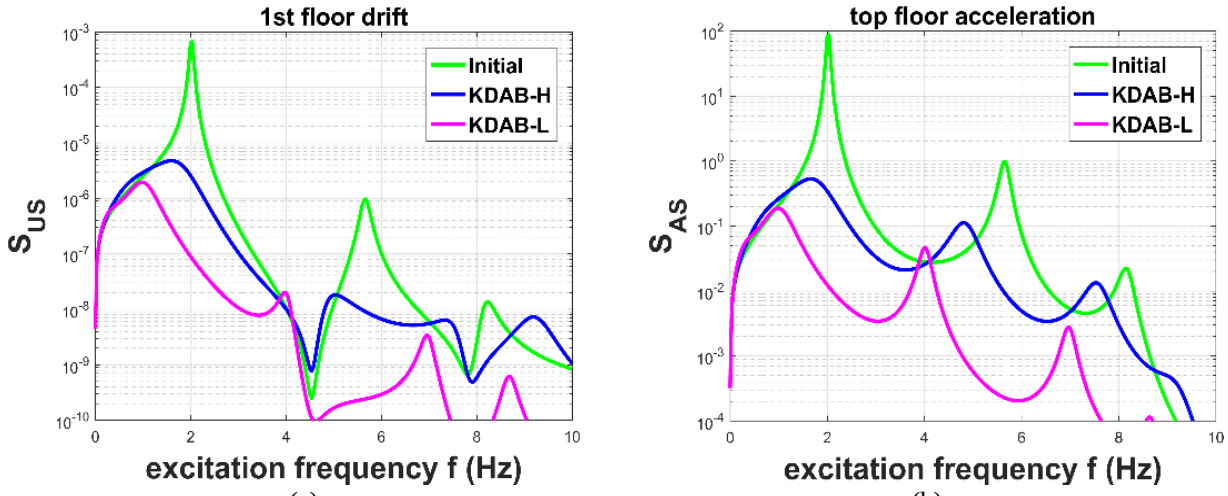

(a) (b)

Figure 8. Response power spectral densities of the structure's critical dynamic responses (a) 1st-floor drift and (b) top floor (3rd) absolute acceleration, of the initial and the KDAB-L and KDAB-H systems.

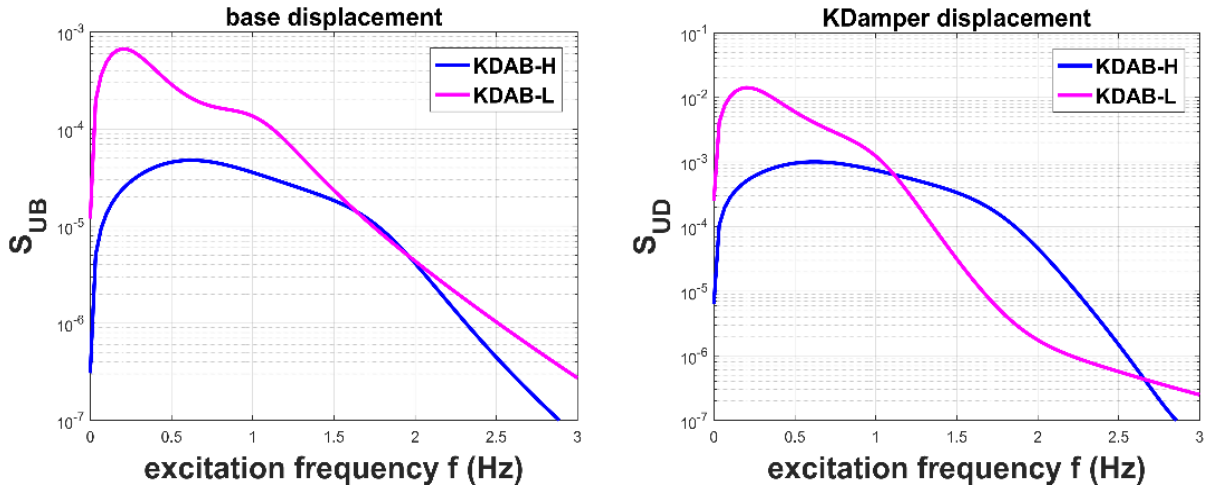

(a) (b)

Figure 9. Response power spectral densities of (a) base's relative displacement and (b) KDamper's relative displacement, of the KDAB-L and KDAB-H systems.

However, although the KDAB-H (f_0=1 *Hz*) represents the same concept with the KDAB-L (f_0=0.4 *Hz*) system, with a stiffer base (higher nominal frequency), it manages to reduce the maximum value of S_{UB} more than one order of magnitude, as compared with the KDAB-L system (Figure 9.a). Finally, by making a stiffer base (KDAB-H), the KDamper's maximum value of the relative displacement power spectral density is reduced more than one order of magnitude (Figure 9.b).

4.3. Effect of the KDamper nominal frequency on the root mean square responses

Figure 10 and 11 present the structure's first-floor drift, top floor absolute acceleration, base relative displacement, and the KDamper's relative displacement mean square responses ratios, which are defined as

$$r_{US} = \frac{R_{US}}{R_{US}(ref)}\ ;\ r_{AS} = \frac{R_{AS}}{R_{AS}(ref)}\ ;\ r_{UB} = \frac{R_{UB}}{R_{US}(ref)}\ ;\ r_{UD} = \frac{R_{UD}}{R_{US}(ref)} \tag{14}$$

where $R_{US}(ref)$ and $R_{AS}(ref)$ pertain to the initial 3-story uncontrolled building structure. $R_{US}(ref)$ is the first floor's maximum relative displacement and $R_{AS}(ref)$ the top (3rd) floor's maximum absolute acceleration. The results concern the KDAB system with parameters μ=5%, κ=3.41, ζ_D=0.622 and a continuous variation of the KDamper's nominal frequency in the range f_0= [0,4 - 1.0] *Hz*. The inherent conflict between the requirement for simultaneous minimization of the structure's absolute acceleration/floor drift and the base's relative displacement is observed.

The KDAB system with a nominal frequency of 0.4 *Hz* (KDAB-L) can be used as a possible supplement to the conventional seismic isolation approaches, significantly improving the superstructure's dynamic performance while retaining the base displacement at acceptable levels, as compared with the classical base isolation concepts. As an alternative, the KDAB can be implemented as a "stiff absorption base" with a much higher nominal frequency (1 *Hz*, KDAB-H system). This way the superstructure's dynamic performance is greatly improved while at the same time the base's relative displacement is in the order of a few centimeters (comparable displacement to a floor drift), as it can be observed in Figures 10 and 11. Finally, the KDamper's relative displacement is greatly reduced as the nominal KDamper frequency increases, as observed in Figure 11.b.

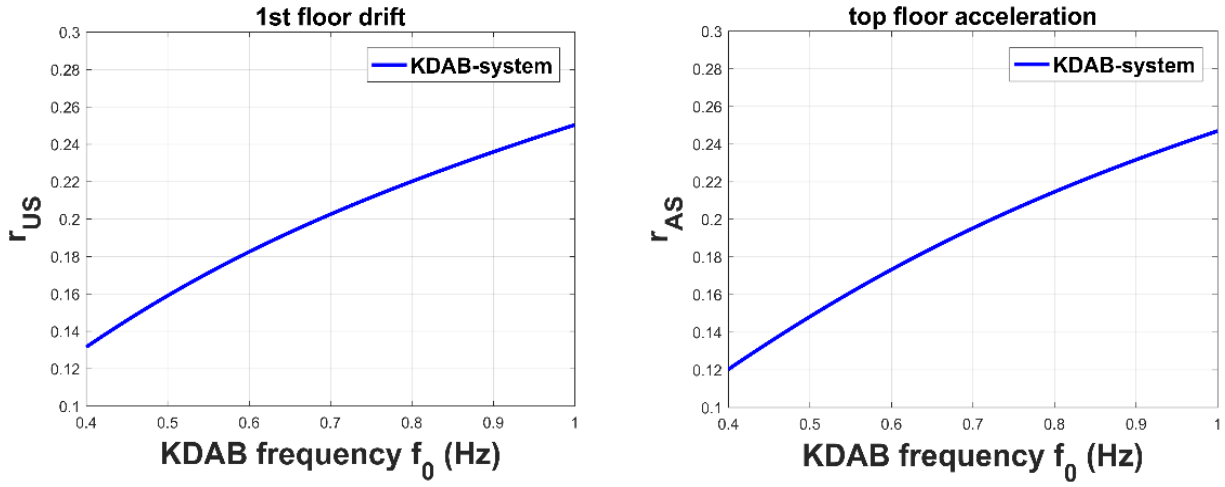

(a) (b)

Figure 10. Root mean square responses ratio (a) of the controlled structure's first-floor drift and (b) structure's top floor (3rd) absolute acceleration, over the nominal KDamper frequency.

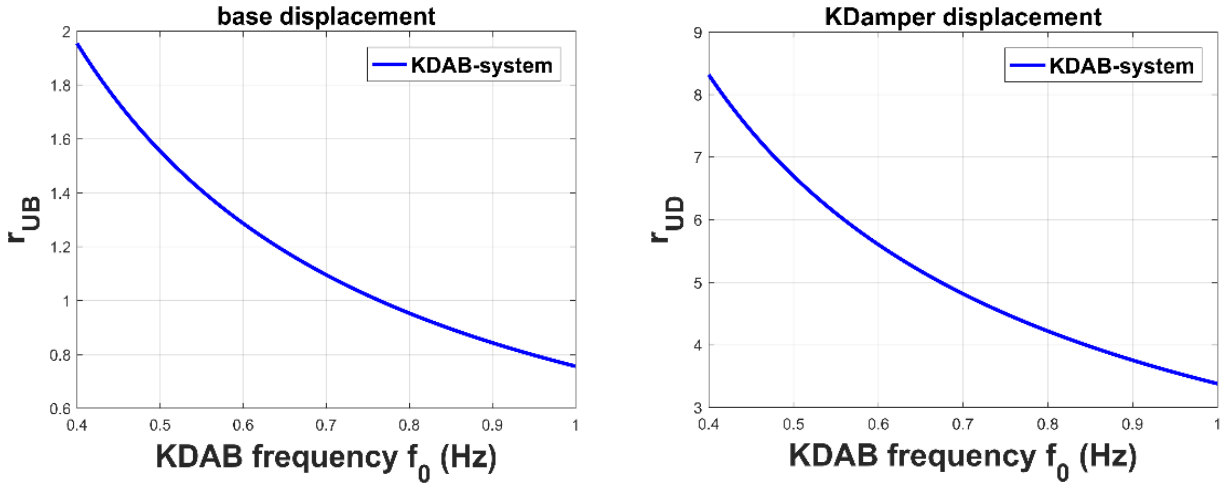

(a) (b)

Figure 11. Root mean square responses ratio (a) of the base's relative displacement and (b) the KDamper's relative displacement, over the nominal KDamper frequency.

5. Numerical Evaluation

5.1. Selection of the system parameters

The KDamper implemented as a "stiff seismic absorption base", mentioned in the previous as KDAB-H system, combines a drastic reduction in the base's relative displacement, combined with an acceptable superstructure dynamic behavior, in terms of floor drifts and absolute accelerations, and therefore will be examined as an alternative to the classical seismic isolation approaches. The parameters for this proposed configuration are presented in Table 1 (KDAB-H system). Considering the test case presented in Section 4.1, the resulting stiffness values, as well as the additional mass and the damping coefficient of the KDAB-H system, are presented in Table 2.

KDamper devices can operate in parallel, and therefore multiple KDamper devices can be placed under each of the structure's columns, as in the case of seismic isolation bearings. For the

considered 3-story concrete building structure, one KDamper device is designed to be placed under each of the structure's columns. Thus, 16 KDamper devices provide the necessary values presented in Table 2. In Table 3 is the full set of parameters for each of the 16 KDamper devices, the realization of each will be discussed below.

Table 2. Stiffness values, additional mass and damping coefficient of the proposed configuration (KDAB-H).

System	m_D (*tn*)	k_R (*kN/m*)	k_D (*kN/m*)	k_N (*kN/m*)	C_D (*kNs/m*)
KDAB-H	14.5	54288	12563	-9714.3	252.82

Table 3. Full set of parameters for each one of the 16 KDamper devices.

μ_i	κ_i	ζ_{Di}	m_D (*tn*)	k_R (*kN/m*)	k_D (*kN/m*)	k_N (*kN/m*)	C_D (*kNs/m*)
0.05	3.41	0.622	0.90625	3393	785.1875	-607.143	15.80125

5.2. Indicative design of the KDamper devices

The selection of the negative stiffness element's set-up as well as the design of the positive stiffness elements and the artificial damper, require the solution of a linear problem first in order to estimate the maximum absolute displacement values that are necessary for the design. More specifically, the internal DoF's (KDamper's) displacement is required for the design of the negative stiffness element, the base's displacement for the positive stiffness element k_R and the relative displacement between the base and the KDamper for the positive stiffness element k_D as well as for the artificial damper c_D. All the aforementioned maximum dynamic response together with the main dynamic responses of the system along with the results of a conventional (5%) and a highly (15%) damped base isolated system are presented in Table 4. The results concern the mean and maximum values of all the 30 Artificial Accelerograms in the database.

Table 4. Dynamic responses of the linear problem.

		Initial	BIS (5%)	BIS (15%)	KDAB-H
1st floor drift (*m*)	Max	0.0628	0.0056	0.0051	0.0165
	Mean	0.0468	0.005	0.0043	0.014
3rd floor abs. acc (m/sec^2)	Max	22.6782	1.7936	1.8674	6.92
	Mean	17.2292	1.5804	1.5794	5.7031
Base displ. (*m*)	Max	-	0.234	0.1967	0.0512
	Mean	-	0.206	0.1616	0.0395
KDamper displ. (*m*)	Max	-	-	-	0.2344
	Mean	-	-	-	0.174
Base-KDamper displ. (*m*)	Max	-	-	-	0.1877
	mean	-	-	-	0.1409

Considering the conventional base isolated system (BIS-5%) simple seismic isolation bearing are selected. In the case of the highly damped (BIS-15%) base isolated system, 8 *SI-S 300/128* elastomeric isolators from the FIP Industrial catalog [35] are selected. The equivalent viscous damping coefficient is 10-15 %, thus a 15% damping ratio is selected for the analysis. Their maximum designed displacement is 25 *cm*, sufficiently greater than the maximum value presented in Table 4 (19.67 *cm*). In both cases (conventional and highly damped base isolated system), the base's frequency (0.4 *Hz*) is designed to be significantly lower than that of the fundamental frequency of the structure ($1/T1$ =1/0.495=2.02 *Hz*).

5.2.1. Realization of the negative stiffness element

Regarding the properties and features of the simple QZS configuration proposed by Carella et al. [13], an alternative mechanism is hereby described, as depicted in Figure 12.

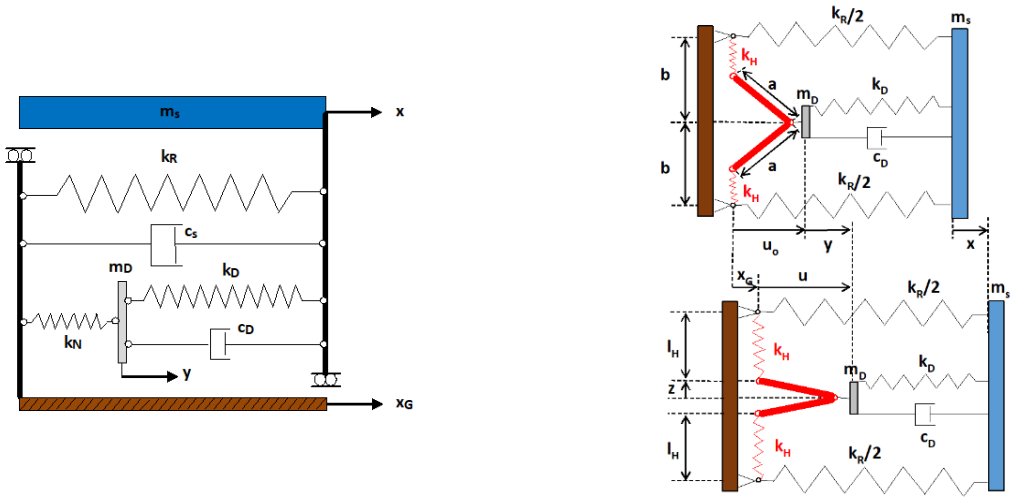

(a) (b)

Figure 12. Schematic representation (a) of the KDamper concept and (b) of the proposed configuration (plan view).

The static equilibrium position and the perturbed position due to an external base dynamic excitation, $x_G(t)$ are both presented in Figure 12.b. The necessary notation concerning the various displacements of the system is also presented. The negative stiffness spring k_N (Figure 12.a) is realized by a set of two symmetric linear horizontal springs with constants k_H, which support the mass m_D by an articulated mechanism. In order to calculate the value of negative stiffness produced by this pair of positive stiffness springs, the ensuing procedure is followed. First, the energy due to the deformation of the springs, k_H is calculated as

$$U_N(u) = 2\frac{1}{2}k_H(l_H - l_{HI})^2 \tag{15.a}$$

$$l_H = b - (a^2 - u^2)^{1/2} \tag{15.b}$$

Then, the elastic non-linear force corresponding to the negative stiffness is given as

$$f_N(u) = \frac{\partial U_N}{\partial u} = \frac{\partial U_N}{\partial u_D} = -2k_H\left(1 + \frac{l_{HI} - b}{\sqrt{a^2 - u^2}}\right)u = -2k_H\left[1 + c_I\frac{1}{(1 - u^2/a^2)^{1/2}}\right]u \tag{16.a}$$

$$u = u_0 + u_D \tag{16.b}$$

$$c_I = (l_{HI} - b)/a \tag{16.c}$$

Finally, the value of the negative stiffness produced by each pair of linear pre-compressed horizontal springs, k_H is given by

$$k_N = \frac{\partial f_N}{\partial u} = \frac{\partial f_N}{\partial u_D} = -2k_H\left[1 + c_I\frac{1}{(1 - u^2/a^2)^{3/2}}\right] \tag{17}$$

In Eq. (15.b), (16.a-c) and (17), a and b are geometrical parameters, as defined in Figure 12.b, while l_{HI} denotes the initial length of the undeformed springs, k_H. The pair of springs k_H generate the negative stiffness element k_N. In the case of $c_I = 0$, two horizontal springs are equivalent to a spring with $k_N = -2k_H$. Next, the parameters of the negative stiffness element and the corresponding

mechanism are selected. The parameter u_0 is selected equal to 0.1 *cm*. This value is close to zero so that an almost symmetric response around $u = 0$ is obtained. The rest of the parameters are selected so that $k_N(0) = 1.01k_{NC}$ and $k_N(umax) = 0.90k_{NC}$, where k_{NC} is the constant negative stiffness of the KDamper device, as presented in Table 4. Since $k_N(u = 0)$ is the minimum value of the negative stiffness element, the system remains statically and dynamically stable (Eq. (A.1)) for the entire operating range. The value of c_I is selected -0.05, in order to achieve as far as possible a linear behavior. Table 5 presents the entire set of parameters of the proposed configuration concerning the negative stiffness element for each one of the sixteen KDamper devices, with k_{NC} = -607.1437 *kN/m*.

Table 5. Negative stiffness spring and mechanism parameters for each one of the sixteen KDamper devices.

k_H (*kN/m*)	l_{HI} (*m*)	a (*m*)	b (*m*)	c_I
322.743	0.504	0.324	0.520	-0.05

Figure 13 presents the variation of the negative stiffness, of the proposed configuration, over the KDamper's relative displacement. It is observed, that in the range of -0.2344 *m* to +0.2344 *m*, which is the maximum range of the KDamper's relative displacement of all the Artificial Accelerograms in the database, the negative stiffness is pretty much constant.

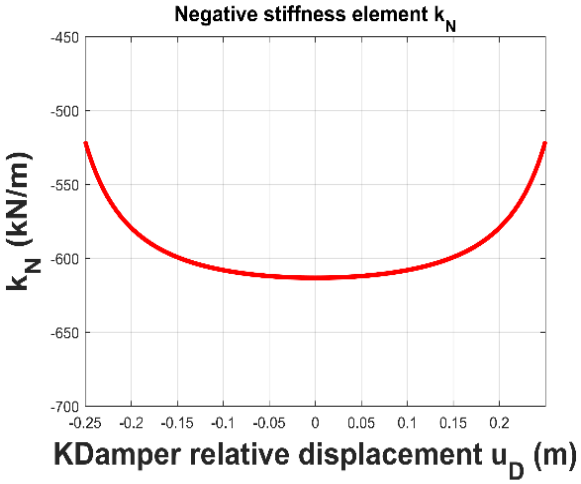

Figure 13. Variation of the negative stiffness, of the proposed configuration, over the KDamper's relative displacement.

5.2.2. Realization of the positive stiffness elements k_R and k_D, artificial damper c_D and additional mass m_D

The material used to realize the additional mass of each of the 16 KDamper devices is steel, with a value of density equal to ρ_{mat} = 7850 kg/m^3. Assuming cubic shape for the additional mass, the resulting dimension of the additional mass of each device is

$$x_{add,mass} = \sqrt[3]{(m_D / No.Columns) / \rho_{mat}} = \sqrt[3]{(14.5/16)/7.85} = 0.487m \quad (18)$$

The maximum relative displacement between the base and the additional mass of the device is 0.1877 *m*. Therefore, conventional spiral springs can be used in the making of the positive stiffness element k_D. Each one of the sixteen KDamper's artificial damper coefficient is low (15.8 *kNs/m*), so common linear damping devices can be used, as for example Catalog No./Model LD720 from ITT Infrastructure viscous dampers catalog [36], with a designed maximum stroke of 20 *cm* and a total initial length of 52.2 *cm*.

The positive stiffness element k_R works totally independent from the other stiffness elements, the additional mass, and the artificial damper, as shown in Figure 5.a. Thus, there are numerous alternatives for the realization of k_R, the design of which is beyond the scope of the current paper. Some realistic examples are for instance simple elastomeric bearings or steel simply supported cantilever beams. Finally, a schematic representation of the proposed configuration with all the resulting dimensions of the KDamper parameters is given in Figure 14.

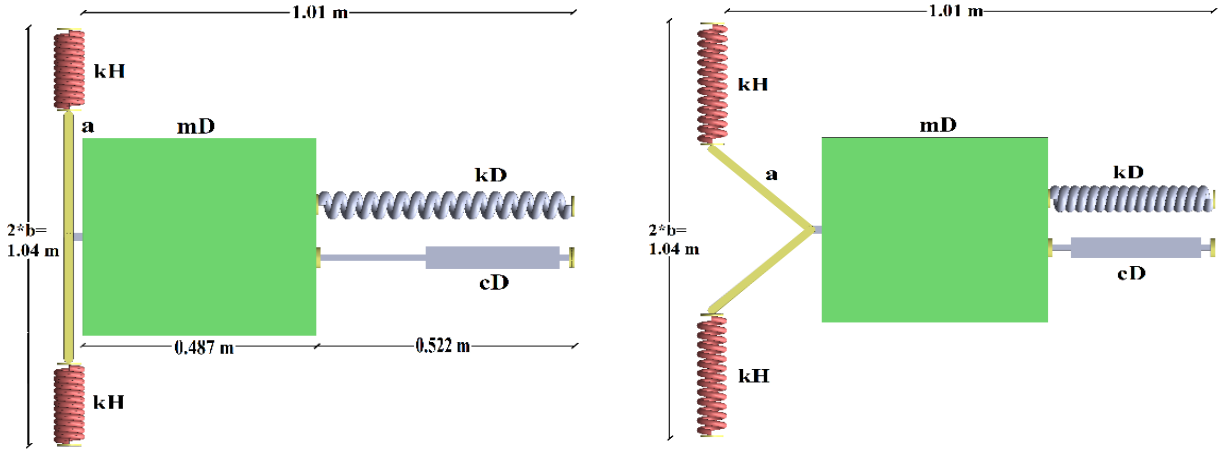

Figure 14. Schematic representation (plan view) of the proposed configuration of the KDamper concept (a) undeformed state and (b) deformed state.

5.3. Numerical results

The system of non-linear equations, of the KDAB-H system with non-linear negative stiffness, k_N, is solved using the Newmark-β method with linear accelerations. Figure 15 and 16 present comparative results between the linear problem solved in Section 5.1 and the proposed non-linear configuration in 5.2, regarding the internal KDamper displacement (relative to the ground), the base displacement and the 1st floor drift, for a random artificial accelerogram of the database. It is proven that the results of the proposed non-linear system are in a very good agreement to that of the linear one previously solved.

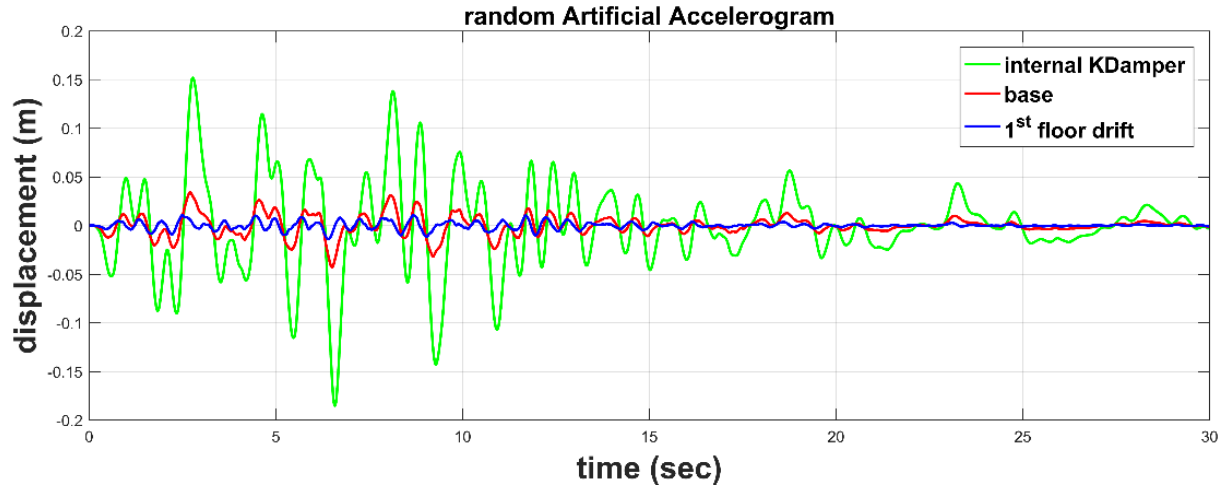

Figure 15. Dynamic responses of the isolated linear system, internal KDamper displacement, base displacement and 1st-floor drift in m ($\max|u_{KD}| = 0.1853\ m$, $\max|u_{base}| = 0.0427\ m$, $\max|u_{drift}| = 0.0141\ m$).

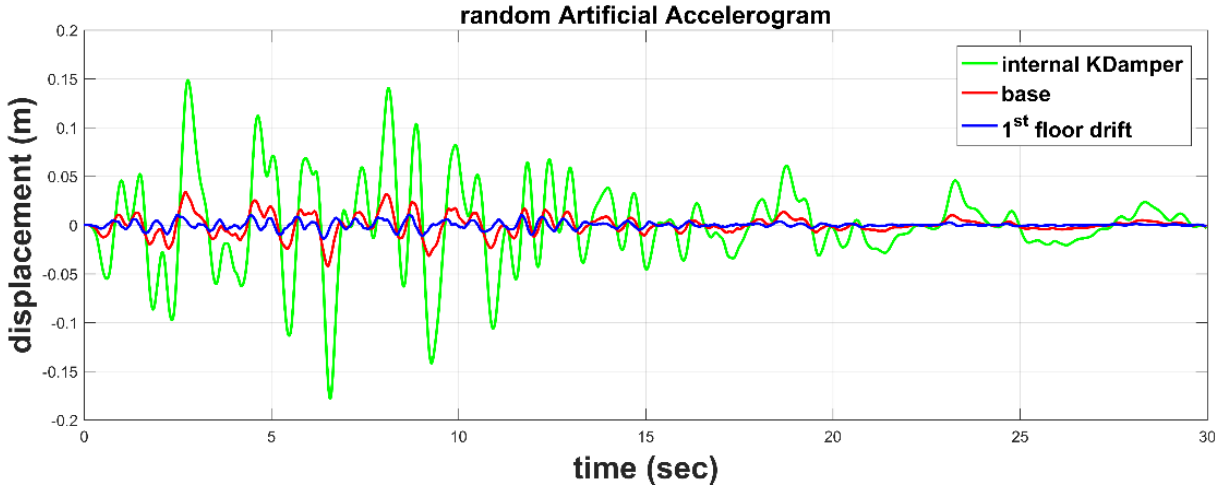

Figure 16. Dynamic responses of the isolated non-linear system, internal KDamper displacement, base displacement and 1st-floor drift in m ($\max|u_{KD}| = 0.1783\ m$, $\max|u_{base}| = 0.0421\ m$, $\max|u_{drift}| = 0.0140\ m$).

Real earthquake ground motions do not have smoothed spectra nor a fixed duration. Therefore, it is of utmost importance to scrutinize the effectiveness of the proposed vibration control strategy also with real accelerograms, recorded in earthquakes. Seven natural earthquake signals are investigated: Northridge, El Centro, Kobe, L'Aquila, Tabas, Aigio and Kalamata, with their PGA and duration presented in Table 6. The mean PGA of the 30 artificial accelerograms of the database is 0.519 *g*.

Table 6. PGA and duration of investigated real earthquake records.

	Northridge	ElCentro	Kobe	L'Aquila	Tabas	Aigio	Kalamata
PGA (*g*)	0.43	0.35	0.28	0.34	0.85	0.54	0.24
Duration (*sec*)	26.58	53.74	32	40	32.28	30.1	29.24

The systems main responses, considering max values of the dynamic responses for all the artificial accelerograms in the database (mean of 30 max), as well as the selected real earthquake records in this paper, of the initial (IN) 3-story concrete building structure, the highly damped base isolated system (BIS (15%)) and the controlled structure with the KDamper implemented as a "stiff absorption base" (KDAB-H (1 *Hz*)) are presented in Table 7, 8 and 9. Comparative results between the initial, the highly damped base isolated system (BIS-15%) and the KDAB with a nominal frequency f_0=1 *Hz* (KDAB-H), are presented in Figure 17. The presented time histories relate to two real earthquake records: L'Aquila and Tabas.

Table 7. List of structure's top floor (3rd) absolute acceleration, considering max values of the dynamic responses, and the *%* reduction compared to the initial 3-story top floor accelerations.

System	Earthquake excitation							
	Artificial	Northridge	ElCentro	Kobe	L'Aquila	Tabas	Aigio	Kalamata
Initial	17.23	13.07	13.67	6.65	6.36	30.16	23.93	7.75
BIS	1.58	1.98	1.11	1.87	1.17	4.120	0.97	0.78
(%)	**-90.83**	**-84.85**	**-91.88**	**-71.88**	**-81.60**	**-86.34**	**-95.95**	**-89.94**
KDAB-H	5.701	7.69	4.97	5.18	2.91	10.27	8.43	3.04
(%)	**-66.91**	**-41.16**	**-63.64**	**-22.11**	**-54.25**	**-65.95**	**-64.77**	**-60.77**

Table 8. List of structure's first-floor drift, considering max values of the dynamic responses, and the % reduction compared to the initial 3-story first-floor drift.

System	Earthquake excitation							
	Artificial	Northridge	ElCentro	Kobe	L'Aquila	Tabas	Aigio	Kalamata
Initial	0.0468	0.033	0.0328	0.0209	0.0166	0.0707	0.0614	0.0208
BIS	0.0043	0.0054	0.0033	0.0059	0.0029	0.0108	0.0026	0.0024
(%)	**-90.81**	**-83.64**	**-89.94**	**-71.77**	**-82.53**	**-84.72**	**-95.76**	**-88.46**
KDAB-H	0.014	0.021	0.0149	0.0161	0.0078	0.023	0.0211	0.0085
(%)	**-70.08**	**-36.36**	**-54.57**	**-22.97**	**-53.01**	**-67.47**	**-65.63**	**-59.13**

Table 9. List of structure's base relative displacement, considering max values of the dynamic responses, and the % reduction compared to highly damped base isolated system base's relative displacement.

System	Earthquake excitation							
	Artificial	Northridge	ElCentro	Kobe	L'Aquila	Tabas	Aigio	Kalamata
BIS	0.1616	0.2121	0.1281	0.2235	0.1072	0.3693	0.0834	0.0907
KDAB-H	0.0398	0.0581	0.0273	0.0569	0.0286	0.0646	0.0374	0.0246
(%)	**-75.37**	**-72.61**	**-78.69**	**-74.54**	**-73.32**	**-82.51**	**-55.16**	**-72.88**

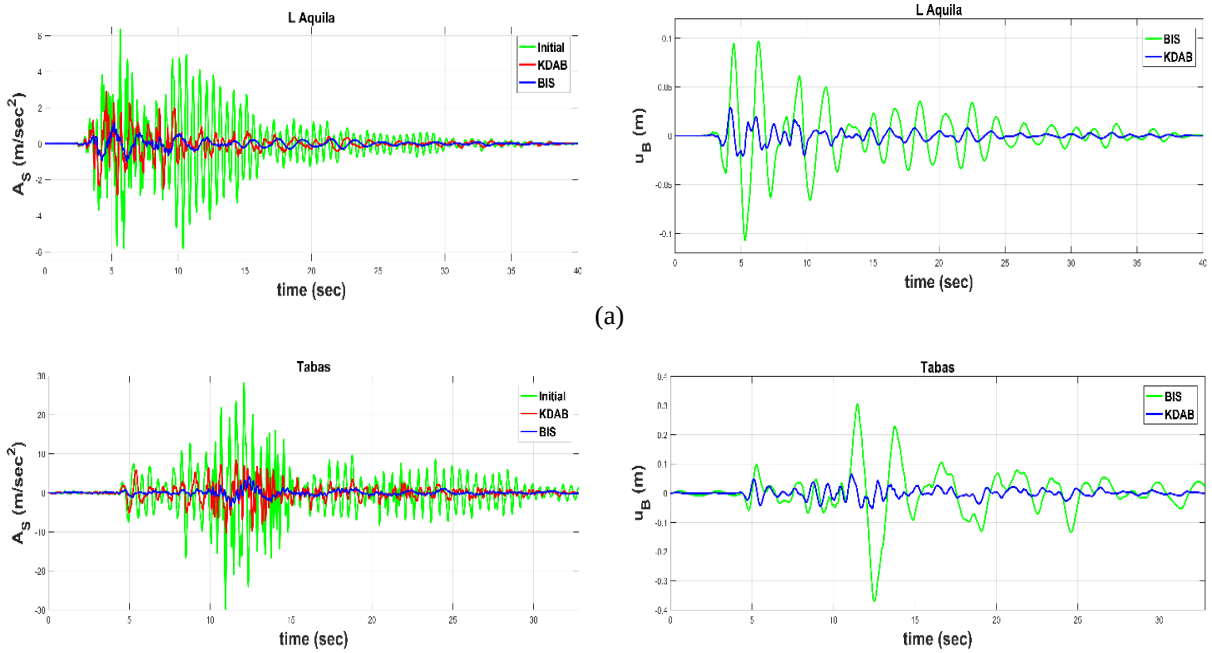

Figure 17. Comparative results in terms of structure's top floor absolute acceleration (*m/sec*^{2}) and base's displacement (*m*), between the initial, the highly damped BIS (15%) and the KDAB-H system, for the (a) L'Aquila and (b) Tabas earthquake.

6. Conclusions

In this paper, the KDamper is implemented for seismic protection in a typical 3-story concrete building structure, as an alternative or supplement of a conventional seismic isolation base. A systematic analytical approach for the selection of the KDamper parameters for acceleration optimization, under base excitation, is considered. A spectra driven optimization of the KDamper

nominal frequency is proposed. The proposed configuration is numerically evaluated in the time domain and the following conclusive comments can be made

i. The optimal design of the KDamper, for optimization of the structure absolute acceleration transfer function, provides an improved dynamic behavior, as compared to other transfer functions previously used.
ii. A compatible ground motion excitation acceleration PSD, generated from a database of artificial accelerograms, can be used to define the root mean square responses. The results confirm the ability of the root mean square responses to represent accurately the effect of the variation of the nominal KDamper frequency to the system maximum dynamic responses.
iii. The indicative design of the KDamper devices proves that the additional mass, the artificial damper, and the stiffness elements, of each implemented device, are within reasonable technological capabilities.
iv. Following the proposed procedure for the realization of the negative stiffness element, the results of the non-linear problem are in a very good agreement to that of the initial linear problem.
v. The KDamper can be implemented effectively as an alternative to the conventional seismic isolation approaches, achieving reductions of more than 50% to the superstructure's dynamic responses, as compared to the initial system, while retaining the base displacement in the order of a few centimeters, 70% lower as compared to the highly damped base isolated system.

According to the above comments, the KDamper concept is a realistic alternative to the existing seismic isolation approaches for building structures, regarding not only horizontal seismic excitations but also vertical ones, due to the ability of the KDamper device to be placed at either horizontal or vertical direction. The reliability and simplicity of the system are also advantages that render the device suitable for various technological implementations and competitive against conventionally used seismic isolation bearings.

Finally, the inherent non-linear nature of the negative stiffness force can be exploited to offer potential advantages of the KDamper concept, such as robustness, broadband response, and energy sinks.

7. Acknowledgments

This research is co-financed by Greece and the European Union (European Social Fund- ESF) through the Operational Programme «Human Resources Development, Education and Lifelong Learning» in the context of the project "Strengthening Human Resources Research Potential via Doctorate Research" (MIS-5000432), implemented by the State Scholarships Foundation (IKY).

References

[1] F. Naeim and J. M. Kelly, Design of seismic isolated structures : from theory to practice. John Wiley, 1999.

[2] M. M. N. Farag, S. S.F. Mehanny, and M. M. Bakhoum, Establishing optimal gap size for precast beam bridges with a buffer-gap-elastomeric bearings system, Earthq. Struct., vol 9, no. 1, pp. 195-219, 2015.

[3] H. Frahm, Device for damping of bodies, US patent #989958, 1911.

[4] J. P. Den Hartog, Mechanical Vibrations, 4th ed. New York, 1956.

[5] L. Qin, W. Yan, and Y. Li, Design of frictional pendulum TMD and its wind control effectiveness, J.

Earthq. Eng. Eng. Vib., vol 29, no. 5, pp. 153-157, 2009.

[6] R. J. McNamara, Tuned Mass Dampers for Buildings, J. Struct. Div., vol 103, no. 9, pp. 1785-1798, 1977.

[7] R. W. Luft, Optimal Tuned Mass Dampers for Buildings, J. Struct. Div., vol 105, no. 12, pp. 2766-2772, 1979.

[8] T. Haskett, B. Breukelman, J. Robinson, and J. Kottelenberg, Tuned mass dampers under excessive structural excitation, Rep. Motioneering Inc, 2004.

[9] N. Debnath, S. K. Deb, and A. Dutta, Multi-modal vibration control of truss bridges with tuned mass dampers under general loading, JVC/Journal Vib. Control, vol 22, no. 20, pp. 4121-4140, 2016.

[10] B. Weber and G. Feltrin, Assessment of long-term behavior of tuned mass dampers by system identification, Eng. Struct., vol 32, no. 11, pp. 3670-3682, 2010.

[11] W. Molyneaux, Supports for Vibration Isolation. G. Britain: ARC/CP-322, Aer Res Council, 1957.

[12] D. L. Platus, Negative-stiffness-mechanism vibration isolation systems, in Proc. of SPIE, 1992, vol. 1619, pp. 44-54, 1992.

[13] A. Carrella, M. J. Brennan, and T. P. Waters, Static analysis of a passive vibration isolator with quasi-zero-stiffness characteristic, J. Sound Vib., vol 301, no. 3-5, pp. 678-689, 2007.

[14] R. A. Ibrahim, Recent advances in nonlinear passive vibration isolators, J. Sound Vib., vol 314, no. 3-5, pp. 371-452, 2008.

[15] J. Winterflood, D. Blair, and B. Slagmolen, High performance vibration isolation using springs in Euler column buckling mode, Phys. Lett. A, vol 300, no. 2-3, pp. 122-130, 2002.

[16] L. N. Virgin, S. T. Santillan, and R. H. Plaut, Vibration isolation using extreme geometric nonlinearity, J. Sound Vib., vol 315, no. 3, pp. 721-731, 2008.

[17] S. Nagarajaiah, D. T. R. Pasala, A. Reinhorn, M. Constantinou, A. A. Sarlis, and D. Taylor, Adaptive Negative Stiffness: A New Structural Modification Approach for Seismic Protection, Adv. Mater. Res., vol 639-640, pp. 54-66, 2013.

[18] R. DeSalvo, Passive, Nonlinear, Mechanical Structures for Seismic Attenuation, J. Comput. Nonlinear Dyn., vol 2, no. 4, pp. 290, 2007.

[19] H. Iemura and M. H. Pradono, Advances in the development of pseudo-negative-stiffness dampers for seismic response control, Struct. Control Heal. Monit., vol 16, no. 7-8, pp. 784-799, 2009.

[20] N. Attary et al., Application of Negative Stiffness Devices for Seismic Protection of Bridge Structures, Proc. 2012 ASCE Str. Congr., pp. 506-515, 2012.

[21] N. Attary et al., Performance Evaluation of a Seismically-Isolated Bridge Structure with Adaptive Passive Negative Stiffness, Proc of 15th WCEE, Lisbon, Portugal, September, 2012.

[22] D. T. R. Pasala, A. A. Sarlis, S. Nagarajaiah, A. M. Reinhorn, M. C. Constantinou, and D. Taylor, Negative Stiffness Device for Seismic Response Control of Multi-Story Buildings, in 20th Analysis and Computation Specialty Conference - Proceedings of the Conference, pp. 83-96, 2012.

[23] A. A. Sarlis, D. T. R. Pasala, M. C. Constantinou, A. M. Reinhorn, S. Nagarajaiah, and D. P. Taylor, Negative Stiffness Device for Seismic Protection of Structures, in Journal of Structural Engineering, Corfu, Greece, vol 139, no. 7, pp. 1124-1133, 2012.

[24] A. A. Sarlis, D. T. R. Pasala, M.C. Constantinou, A. M. Reinhorn, S. Nagarajaiah, and D. P. Taylor, Negative Stiffness Device for Seismic Protection of Structures: Shake Table Testing of a Seismically Isolated Structure, J. Struct. Eng., 2016.

[25] I. A. Antoniadis, S. A. Kanarachos, K. Gryllias, and I. E. Sapountzakis, KDamping: A stiffness based vibration absorption concept, JVC/Journal Vib. Control, vol. 24, no. 3, pp. 588-606, 2018.

[26] I. A. Antoniadis, I. E. Sapountzakis and E. F. Chatzi, A KDAMPING CONCEPT FOR SEISMIC EXCITATION ABSORPTION, in In: Proc of the 1st ICONHIC 2016.

[27] E. J. Sapountzakis, P. G. Syrimi, and I. A. Antoniadis, KDamper Concept in Seismic Isolation of Bridges, in In: Proc of the 1st ICONHIC 2016, Chania, Crete, Greece, pp. 28-30, 2016.

[28] E. J. Sapountzakis, P. G. Syrimi, I. A. Pantazis, and I.A. Antoniadis, KDamper concept in seismic isolation of bridges with flexible piers, Eng. Struct., vol. 153, pp. 525-539, 2017.

[29] K. A. Kapasakalis, I. A. Antoniadis and E. J. Sapountzakis, Kdamper concept in seismic isolation of building structures with soil structure interaction, in The 13th International Conference on Computational Structures Technology (CST2018), 2018.

[30] P. Syrimi, E. Sapountzakis, G. Tsiatas, and I. Antoniadis, Parameter Optimization of the Kdamper Concept in Seismic Isolation of Bridges Using Harmony Search Algorithm, in In: Proc of the 6th COMPDYN 2017, Rhodes Island, Greece, pp. 37-51, 2017.

[31] A. Giaralis and P. D. Spanos, Derivation of response spectrum compatible non-stationary stochastic processes relying on Monte Carlo-based peak factor estimation, Earthq. Struct., vol. 3, no. 3-4, pp. 581-609, 2012.

[32] P. Cacciola and L. D'Amico, Response-Spectrum-Compatible Ground Motion Processes, in Encyclopedia of Earthquake Engineering, pp. 1-27, 2015.

[33] Seismosoft [2018], SeismoArtif - A computer program for generating artificial earthquake accelerograms matched to a specific target response spectrum, 2018. [Online]. Available: http://www.seismosoft.com.

[34] G. R. Saragoni and G. C. Hart, Simulation of artificial earthquakes, Earthq. Eng. Struct. Dyn., vol. 2, no. 3, pp. 249-267, 1973.

[35] Elastomeric isolators - Fip Industriale. [Online]. Available: https://www.fipindustriale.it/index.php?area=106&menu=67&lingua=1. [Accessed: 13-May-2019].

[36] Fluid Viscous Dampers | Seismic Dampers | ITT Infrastructure | ITT Enidine. [Online]. Available: http://itt-infrastructure.com/en-US/Products/Viscous-Dampers/. [Accessed: 13-May-2019].

Appendix A: The KDamper Concept

Figure A.1 presents the basic layout of the vibration isolation and damping concept considered the KDamper concept. The device is designed to minimize the response $x(t)$ of an undamped SDoF system of mass m and static stiffness k of to a base excitation of $x_G(t)$. Similar to the Negative Stiffness (NS) isolators, it uses a negative stiffness element k_N.

(a) (b)

Figure A.1. (a) Undamped (or low damped) SDoF system and (b) schematic representation of the KDamper concept.

However, contrary to the NS isolators, the first basic requirement of the KDamper is that the overall static stiffness of the system is maintained

$$k_R + \frac{k_P k_N}{k_P + k_N} = k \tag{A.1}$$

The equations of motion after the implementation of the KDamper are presented below

$$m\ddot{u}_S + k_R u_S + m_D \ddot{u}_D + k_N u_D = -(m + m_D) a_G \tag{A.2.a}$$

$$m_D \ddot{u}_D - c_D(\dot{u}_S - \dot{u}_D) - k_P(u_S - u_D) + k_N u_D = -m_D a_G \tag{A.2.b}$$

Assuming a harmonic excitation in the form of $a_G(t)=A_G e^{j\omega t}$ and steady-state responses of $u_S(t) = \tilde{U}_S \exp(j\omega t)$ and $u_D(t) = \tilde{U}_D \exp(j\omega t)$, the equations of motion, Eq. (A.2) of the KDamper becomes

$$-\omega^2 m\tilde{U}_S + k_R\tilde{U}_S - \omega^2 m\tilde{U}_D + k_N\tilde{U}_D = -(m + m_D)A_G \tag{A.3.a}$$

$$-\omega^2 m_D\tilde{U}_D - j\omega c_D(\tilde{U}_S - \tilde{U}_D) - k_P(\tilde{U}_S - \tilde{U}_D) + k_N\tilde{U}_D = -m_D A_G \tag{A.3.b}$$

A careful examination of Eq. (A.3) reveals that the amplitude F_{MD} of the inertia force of the additional mass and the amplitude F_N of the negative stiffness force

$$F_{MD} = -\omega^2 m_D \left|\tilde{U}_D\right|;\ F_N = k_N \left|\tilde{U}_D\right| \le 0 \tag{A.4.a, b}$$

are exactly in phase, due to the negative value of k_N. Thus, the KDamper can be considered as an indirect approach to increase the inertia effect of the additional mass m_D without however increasing directly the mass m_D itself. Moreover, it should be noted that the value of F_{MD} depends on the frequency, while the value of F_N is constant in the entire frequency range, a fact which is of importance for low-frequency vibration isolation.

A.1 Basic properties of the KDamper

A first fundamental property of KDamper is that the addition of a negative stiffness spring reduces the magnitude of the transfer function, as compared to that of a TMD with the same value of μ, as observed in Figure A.2. The increase in the value of κ is upper limited by a value of κ_{max}. As observed in Figure A.3.a, when κ reaches κ_{max} the frequency ratio ρ tends to infinity. At the same time, (Fig. A.3.b) transfer function H_{ASI} of the KDamper tends to zero.

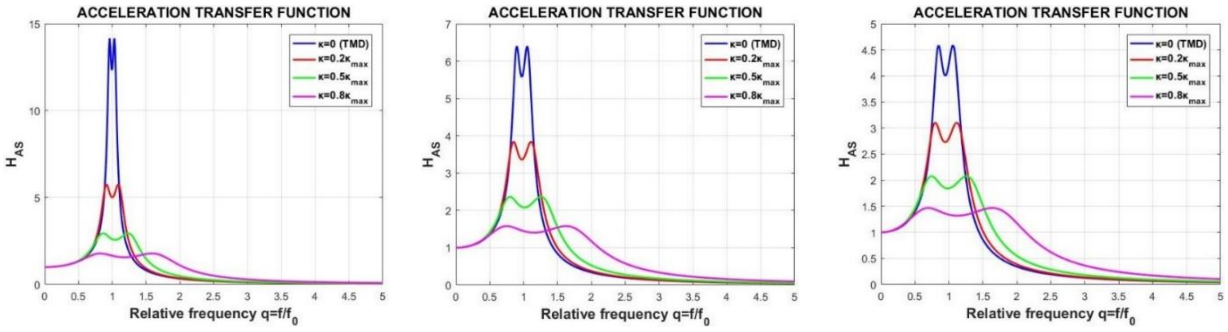

(a) (b) (c)

Figure A.2. Effect of the stiffness ratio κ on the transfer function H_{AS} of the KDamper for (a) μ=0.01, (b) μ=0.05 and (c) μ=0.10.

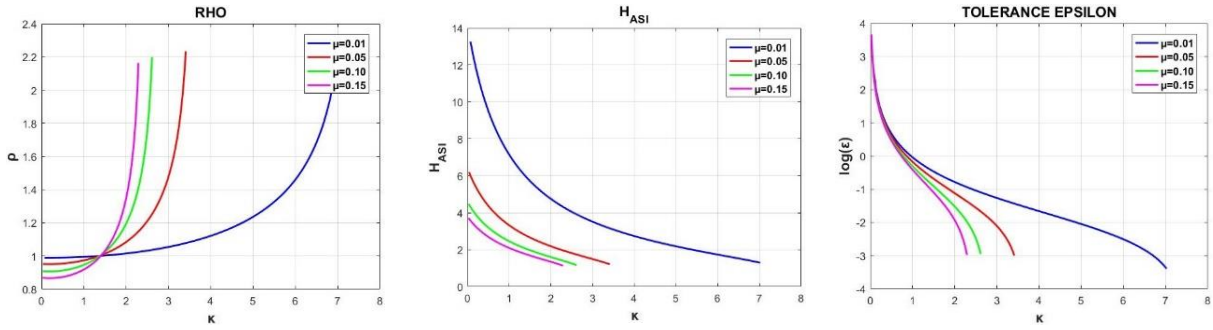

(a) (b) (c)

Figure A.3. Effect of the variation of the κ and μ KDamper parameters on (a) the value of $\rho=\omega_D/\omega_0$, (b) the value H_{ASI} of the transfer function at the invariant points q_L, q_R and (c) the static stability margin ε.

Increasing κ has a number of implications in the design of the KDamper. From a dynamics point of view, the transfer function tends to present a more broadband behavior, as observed in Figure A.2. From a technological point of view, increasing κ results in high stiffness values of the internal KDamper elastic elements, as presented in Figure A.4. An increase of the absolute value of k_N by a factor ε may lead to a new value of k_{NL} where the structure becomes unstable

$$k_R + \frac{k_P k_{NL}}{k_P + k_{NL}} = 0 \Leftrightarrow k_{NL} = -\frac{k_R k_P}{k_R + k_P} = (1+\varepsilon)k_N \tag{A.5}$$

Substitution of Eq. (B.16.a) into (A.5) leads to the following estimate for the static stability margin $\varepsilon=1/(\kappa[(1+(1+\kappa)^2\,\mu\rho^2])$. Figure A3.c presents the variation of ε over κ and μ. As it can be observed, the increase of the negative stiffness of the system is upper bounded by the static stability limit of the structure, where ε tends to zero.

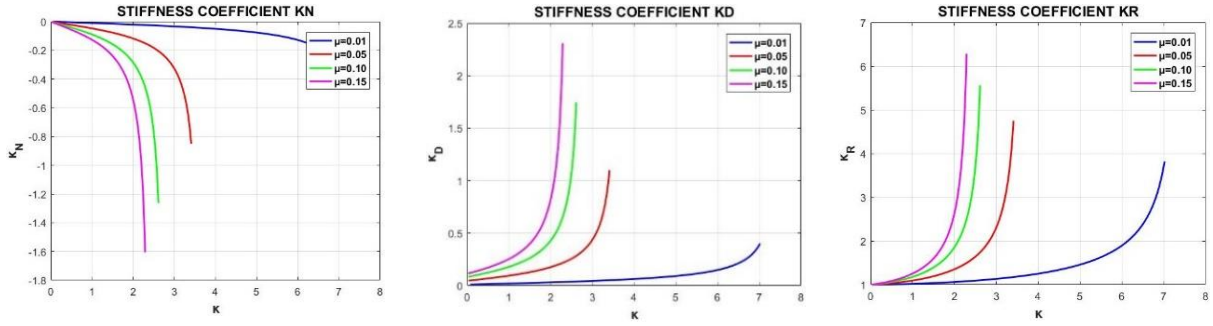

(a) (b) (c)

Figure A.4. Effect of increasing κ on the values of stiffness elements of the KDamper. (a) κ_N, (b) κ_P and (c) κ_R.

Appendix B: Selection of the KDamper Parameters for Optimal Acceleration Response Under Base Excitation

A number of Transfer Functions of the KDamper result from Eq. (A.3)

$$\tilde{H}_{US} = \frac{\tilde{U}_S}{A_G} = -\frac{\tilde{N}_{US}}{\tilde{D}}\,;\; \tilde{H}_{UD} = \frac{\tilde{U}_D}{A_G} = \frac{(j\omega c_D + k_P)\tilde{H}_{US} - m_D}{(-\omega^2 m_D + j\omega c_D + k_p + k_N)} = \frac{\tilde{N}_{UD}}{\tilde{D}}\,;$$
$$\tilde{H}_{AS} = \frac{\tilde{A}_S}{A_G} = 1 - \omega^2 \tilde{H}_{US} = \frac{\tilde{N}_{AS}}{\tilde{D}} \tag{B.1}$$

where

$$\tilde{N}_{US} = -\omega^2 m m_D + j\omega c_D (m + m_D) + m(k_P + k_N) + m_D k_P \tag{B.2.a}$$

$$\tilde{N}_{UD} = -\omega^2 m m_D + j\omega c_D (m + m_D) + m k_P + m_D (k_R + k_P) \quad \text{(B.2.b)}$$

$$\tilde{N}_{AS} = -\omega^2 m_D k_R + j\omega c_D (k_R + k_N) + k(k_P + k_N) \quad \text{(B.2.c)}$$

$$\tilde{D} = \omega^4 m m_D - j\omega^3 (m + m_D) c_D - \omega^2 (m + m_D)(k_P + k_R) + j\omega c_D (k_R + k_N) + k(k_P + k_N) \quad \text{(B.2.d)}$$

where k is the total initial static stiffness of the system, as described in Eq. (A.1). The procedure for the optimal selection of the KDamper parameters follows the classical minmax ($H\infty$) approach, first proposed by Den Hartog [4]. Eq. (B.1) are brought to a non-dimensional form with respect to the natural frequency of the system ω_0, using the following parameters

$$\kappa = -k_N / (k_P + k_N) \; ; \; \mu = m_D / m \quad \text{(B.3.a)}$$

$$\rho = \omega_D / \omega_0 \; ; \; q = \omega / \omega_0 \; ; \; \omega_0 = \sqrt{k / m} \; ; \; \omega_D = \sqrt{k_D / m_D} \; ; \; \zeta_D = c_D / 2\sqrt{k_D m_D} \quad \text{(B.3.b)}$$

As a result, $\tilde{H}_{AS}$ of Eq. (B.1) can be written in the form

$$\tilde{H}_{AS} = -\frac{A + (j2\zeta_D)B}{C + (j2\zeta_D)D} \; ; \; H_{AS} = \frac{|\tilde{A}_S|}{A_G} = \frac{A_S}{A_G} = \sqrt{\frac{A^2 + (2\zeta_D)^2 B^2}{C^2 + (2\zeta_D)^2 D^2}} \quad \text{(B.4.a, b)}$$

In the limit cases of ζ_D=0 or $\zeta_D \to \infty$, H_{AS} of Eq. (B.4) becomes

$$H_{AS}(0) = \left|\frac{A}{C}\right| \; ; \; H_{AS}(\infty) = \left|\frac{B}{D}\right| \quad \text{(B.5.a, b)}$$

The acceleration transfer function $H_{AS}(q,\zeta_D)$ of Eq. (B.4) has two poles for two different values of q and therefore, it presents two different maximal values (peaks) at these points. The optimal selection of the parameters of the KDamper requires that both these peaks are minimized and become equal to each other. The approach is based on the identification of a pair of frequencies q_L <1 and q_R>1, where the values $H_{AS}(q_L)$ and $H_{AS}(q_R)$ become independent of ζ_D. The first step for the optimization procedure is the requirement that the values of the transfer functions at these points are equal

$$H_{AS}(q_L) = H_{AS}(q_R) = H_{ASI} = H_{AS}(\infty) \quad \text{(B.6)}$$

In order that a solution for such a pair of frequencies exist, two alternative conditions must be fulfilled

Case I: $$AD = BC \quad \text{(B.7.a)}$$

Case II: $$AD = -BC \quad \text{(B.7.b)}$$

As can be verified, no solution to Eq. (B.7.a) exists for a positive q^2, when the values κ, μ, and ρ are positive. Elaboration of Eq. (B.7.b) results to

$$(A_2 D_2 + B_0) q^4 + (A_0 D_2 + A_2 D_0 + B_0 C_2) q^2 + (A_0 D_0 + B_0 C_0) = 0 \quad \text{(B.8)}$$

where

$$A = A_2 q^2 + A_0 \; ; \; B = B_0 \rho q \; ; \; C = q^4 + C_2 q^2 + C_0 \; ; \; D = (D_2 q^2 + D_0) \rho q \quad \text{(B.9)}$$

$$A_2 = A_{2\rho}\rho^2 + A_{20} \; ; \; A_0 = A_{0\rho}\rho^2 + A_{00} \; ; \; B_0 = B_{0\rho}\rho^2 + B_{00} \; ; \; C_2 = C_{2\rho}\rho^2 + C_{20} \quad \text{(B.10.a)}$$

$$C_0 = C_{0\rho}\rho^2 + C_{00} \; ; \; D_2 = D_{2\rho}\rho^2 + D_{20} \; ; \; D_0 = D_{0\rho}\rho^2 + D_{00} \quad \text{(B.10.b)}$$

$$A_\rho = (A_{0\rho} D_{2\rho} + A_{2\rho} D_{0\rho} + B_{0\rho} C_{2\rho}) D_{20} - 2(A_{2\rho} D_{20} + A_{20} D_{2\rho} + B_{0\rho}) D_{0\rho} \quad \text{(B.11.a)}$$

$$B_{\rho A} = [(A_{0\rho} D_{20} + D_{2\rho} A_{00}) + (A_{2\rho} D_{00} + D_{0\rho} A_{20}) + (B_{0\rho} C_{20} + C_{2\rho} B_{00})] D_{20} \quad \text{(B.11.b)}$$

$$B_{\rho B} = -2(A_{2\rho} D_{20} + A_{20} D_{2\rho} + B_{0\rho}) D_{00} - 2(A_{20} D_{20} + B_{00}) D_{0\rho} \quad \text{(B.11.c)}$$

$$B_\rho = B_{\rho A} + B_{\rho B} \quad \text{(B.11.d)}$$

$$C_\rho = (A_{00} D_{20} + A_{20} D_{00} + B_{00} C_{20}) D_{20} - 2(A_{20} D_{20} + B_{00}) D_{00} \quad \text{(B.11.e)}$$

and the coefficients in the Eq. (B.10) are defined in Table B.1.

Table B.1. Coefficients in Equations B.10.

	A_{2i}	A_{0i}	B_{0i}	C_{2i}	C_{0i}	D_{2i}	D_{0i}
i=ρ	$-\kappa(1+\kappa)\mu$	*1*	$\kappa^2\mu$	$-[1+(1+\kappa)^2\mu]$	*1*	*0*	$\kappa^2\mu$
i=0	*-1*	*0*	*1*	*-1*	*0*	$-(1+\mu)$	*1*

As a result of Eq. (B.8), the pair of roots of Eq. (B.8) must satisfy

$$q_L^2 + q_R^2 = -\frac{(A_0 D_2 + A_2 D_0 + B_0 C_2)}{(A_2 D_2 + B_0)} \tag{B.12}$$

Additionally, both roots q_L and q_R must fulfill Eq. (B.5.b), which results in

$$\frac{B_0}{D_0 + D_2 q_L^2} = -\frac{B_0}{D_0 + D_2 q_R^2} \Rightarrow q_L^2 + q_R^2 = -\frac{2D_0}{D_2} \tag{B.13}$$

The combination of Eq. (B.12) and (B.13) leads to an equation for the optimal value of the parameter ρ

$$A_\rho \rho^4 + B_\rho \rho^2 + C_\rho = 0 \tag{B.14}$$

The optimal value of ρ is selected as the minimum positive value of the two roots of Eq. (B.14). The coefficients in Equation (B.4) A, B, C, and D finally result as

$$A = -q^2[1+\kappa(1+\kappa)\mu\rho^2] + \rho^2 \tag{B.15.a}$$

$$B = \rho q(1+\kappa^2\mu\rho^2) \tag{B.15.b}$$

$$C = q^4 - q^2[1+\rho^2+(1+\kappa)^2\mu\rho^2] + \rho^2 \tag{B.15.c}$$

$$D = \rho q[(1+\kappa^2\mu\rho^2) - q^2(1+\mu)] \tag{B.15.d}$$

The corresponding transfer function for the TMD results from Eq. (B.4) by setting κ=0. The Transfer Function in Eq. (B.4) depends now only on four parameters: κ and μ. A straightforward approach for the selection of ζ_D is to calculate it numerically so that it minimizes the peak of the Transfer Function $H_{AS}(q,\zeta_D)$. Figure B.1 presents the variation of $H_{AS}(q,\zeta_D)$ due to the variation of ζ_D.

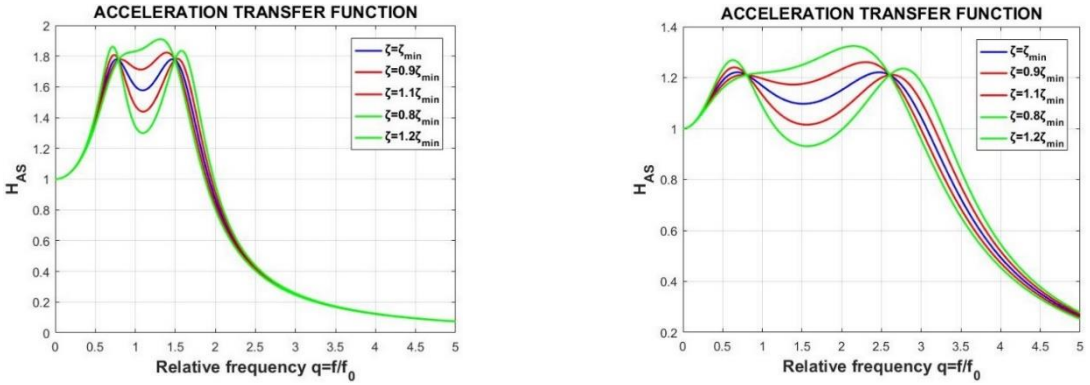

(a) (b)

Figure B.1. Dependence of Transfer Function H_{AS} on the damping ratio ζ_D (a) μ=0.05, κ=2.56 (b) μ=0.05, κ=3.41.

As it can be observed, for the optimum value of $\zeta_{Dopt}=\zeta_{min}$, both peaks of the Transfer Function $H_{AS}(q,\zeta_D)$ are equal and minimum. Once the values of the mass ratio μ and the stiffness ratio κ are known, the values of the elements of the KDamper thus finally result as

$$k_N / k = \kappa_N = -\kappa\mu\rho^2 \; ; \; k_P / k = \kappa_P = (1+\kappa)\mu\rho^2 \; ; \; k_R / k = \kappa_S = 1+\kappa(1+\kappa)\mu\rho^2 \tag{B.16.a}$$

$$m_D = \mu m \; ; \; c_D = 2\zeta_D \sqrt{(k_P + k_N) m_D} \tag{B.16.b}$$

Biographical information

Konstantinos A. Kapasakalis is a PhD candidate at the Institute of Structural Analysis & Antiseismic Research of the Structural Engineering Department of the School of Civil Engineering of the National Technical University of Athens (NTUA). In his PhD, he investigates the seismic protection of structures subjected to dynamic loading under the supervision of Prof. Evangelos Sapountzakis, Prof. Ioannis Antoniadis, and Prof. George Gazetas. His research interests include dynamic analysis of structures, energy dissipation of passive vibration control systems, negative stiffness elements in vibration isolation and higher-order beam theories. He is participating in 2 research projects and he is the author or co-author of 10 reviewed papers in national and international conferences. He has teaching experience as a PhD student in 1 postgraduate and 3 undergraduate courses at NTUA.

Dr. Ioannis A. Antoniadis is a Professor at the School of Mechanical Engineering Department/ NTUA and the Director of the Dynamics and Structures Laboratory. His research interests include dynamic analysis and design of structures and electromechanical systems, smart materials and meta-materials, health monitoring of structures and of large scale cyber-physical systems, monitoring and control of large scale installations and predictive maintenance. He has coordinated or participated as principal researcher in more than 25 international and national research projects. He is the author or co-author of 3 books and academic course notes and of more than 200 reviewed papers in international journals and conferences. He is cooperating for 37 years as a technical project leader/technical consultant with a large number of established Greek and international companies, like Control Data Corporation, GE, Siemens, ABB, ALSTOM, PPC, Aluminium of Greece, Greek Railways, Greek Petroleum, METKA S.A. etc.

Dr. Evangelos J. Sapountzakis is a Professor at the Institute of Structural Analysis and Antiseismic Research of the Structural Engineering Department of the School of Civil Engineering/NTUA. Apart from NTUA, he is also a Professor of Structural Analysis at the School of Corps of Engineers of the Hellenic Army since 1986 and a member of the Coactive Educational Staff of the Hellenic Open University (2011-2017). He has participated in 15 international and national research projects, while in 11 of them as the Principal Investigator. He is the author or co-author of 12 Chapters in books published by International Publishing Companies, 5 Technical Reports, 7 educational books and of more than 280 reviewed papers in international journals and conferences. He is the editor of 4 Books or Conference Proceedings. He has extensive experience (35 years) in the design and analysis of bridge and other large-scale structural projects. His research work has received intentional recognition, since he is Honorary Editor, Editor-in-Chief, Academic Editor, Regional Editor, Associate Editor of international journals and member of the editorial board of 23 international journals.